Test and simulation of dynamic phase compensation from Mita-Teknik A/S

Sørensen, Poul Ejnar; Iov, F.; Blaabjerg, F.; Skaarup, J.

Publication date:
2004

Document Version
Publisher's PDF, also known as Version of record

Risø-R-1438(EN)

Test and simulation of dynamic phase compensation from Mita-Teknik A/S

Poul Sørensen, Florin Iov, Frede Blaabjerg and Jan Skaarup

Risø National Laboratory, Roskilde
March 2004

Abstract This report describes the test of a dynamic phase compensation unit for a wind turbine with directly connected induction generators. The compensation unit is based on thyristor switched capacitors, where conventional wind turbine compensations use mechanical contactors to switch the capacitors. The influence on power quality analysed, and influence on component lifetime is discussed. Besides, simulation models in Matlab/Simulink are presented, including a flickermeter model.

ISBN 87-550-3282-6
ISBN 87-550-3283-4 (Internet)
ISSN 0106-2840

Print: Pitney Bowes Management Services Danmark A/S, 2004

Contents

Preface

This report describes results of the project titled “Dynamic phase compensation”. The project has been funded by the Danish Energy Agency under the UVE program (development program for renewable energy) contract number 51171/01-0009, and it was carried out in cooperation between Mita-Teknik A/S, Risø National Laboratory and Aalborg University.

1 Introduction

Squirrel cage induction generators have traditionally been used in wind turbines, having advantages in costs and robustness. However, one disadvantage of induction machines is that they consume reactive power, which influences the grid integration of the wind turbines in normal operations as well as in the event of faults in the power grid which causes voltage drops at the wind turbine terminal.

Wind turbines with directly connected induction generators are normally equipped with a capacitor bank to fully or partly compensate for the reactive power consumed by the induction generator in normal operation. The capacitors are arranged in smaller groups, which are switched with mechanical contactors one by one.

This report describes a capacitor bank unit developed by Mita-Teknik A/S, using thyristors to switch the capacitor groups. A 317.5 kvar prototype is tested on the 500 kW Nodtank wind turbine in Risø National Laboratory, and simulated in cooperation between Risø and Aalborg University.

The reactive power consumption of the induction generator depends strongly on the active power, which is transmitted by the generator, because of the leakage reactances in the stator and the rotor of the generator. Therefore, the reactive power consumption of the generator fluctuates as the wind speed fluctuates.

Each switching of a capacitor group with a contactor causes transients because the voltages on grid and capacitors are not equal when the contactor is closed. These transients reduce the lifetime of capacitors as well as contactors. To limit the stress of contactors and capacitors, the number of switchings is reduced by the control system, and consequently only the mean value (typically 1-10 minutes mean value) of the reactive power is controlled.

The advantage of applying thyristors instead of mechanical contactors is that the reactive power can be controlled dynamically with a much higher number of switchings and still keep a longer lifetime than with contactor switched capacitors, and moreover, the size of each capacitor group can be selected larger. This is because the switching transients can be significantly reduced when the mechanical contactors are replaced by thyristors, because the switch time can be controlled accurately within a line period, and thus selected at the time when the grid voltage is equal to the capacitor voltage.

The perspective in replacing traditional contactor switched capacitor banks with the dynamic phase compensation unit is first of all to provide better controllability of the reactive power. Depending on the control of the compensation unit, the fast response could be advantageous to reduce the flicker emission from wind turbines, or to support the voltage at the induction generator in the event of a grid fault. In the present work, we have only tested the dynamics during normal operation, and particularly with respect to possible flicker reduction, but the fast response is probably more useful to support the voltage and consequently the ability to ride through grid fault events without disconnection of the wind turbine.

Another perspective of the thyristor concept is to provide more reliable phase compensation. The thyristor based unit can reduce the need for maintenance, which is of particular relevance for off-shore wind turbines.

2 Unit description

The dynamic phase compensation system, developed by Mita-Teknik, is based on phase compensation modules with individual controllers, and the central Mita-Teknik controller including grid measurement module, display and communication interface. The system can be monitored remotely via the communication interface. Likewise, changes in the setup of the system, data logging and upload of new software to the central control unit can be done remotely.

The phase compensation is build as a stand-alone system, which does not interfere with the control system of the Nordtank wind turbine. It is built as 8 modules, 3 × 80 kvar, 1 × 40 kvar, 1 × 20 kvar, 1 × 10 kvar, 1 × 5 kvar and 1 × 2.5 kvar, totally 317.5 kvar. The modules are built together in a way, which ensures that a common forced cooling is established. The central Mita-Teknik control unit performs temperature monitoring and control of fans. The phase compensation system is built into a switchboard.

Each phase compensation module consists of capacitors, thyristors, heat sinks and the module controller. Each module is protected by fuses on the input. The module controller conducts the cut-ins and cut-outs of the capacitors, in order to reduce the switching transients to the possible minimum. The cut-ins and cut-outs are done on request via an ON/OFF signal form the central Mita-Teknik controller. If the capacitor voltage is higher than the grid voltage, a cut-in will be delayed until the capacitor is discharged to the grid voltage. This ensures minimum transients. The module controller returns a status signal to the central Mita-Teknik controller, indicating when all 3 phases are connected.

In contactor switched capacitor banks, choke coils are normally used to reduce the switching transients. In the dynamic phase compensation unit, these choke coils are omitted, because the system is based on low cut-in currents. Initial lab tests in Mita-Teknik indicated that the switching currents were below 1.2 × rated current, even in the worst case where the capacitors are completely discharged at cut-in. However, the size of the transients depends on the grid where the unit is connected, and the test at Risø where the unit is connected to a highly inductive grid, the current transients are a little higher when the capacitor is discharged at cut-in. There are no voltage transients at cut-ins and cut-outs, as the cut-ins take place when the instantaneous grid voltage is equal to the capacitor voltage, and the cut-out takes place when the thyristor current is zero.

The central Mita-Teknik unit controller makes the necessary calculations on, which modules should be cut-in and cut-out, based on measurements done by the grid module and the selected control strategy. Cut-ins and cut-outs of the modules takes place in parallel, so that if e.g. one large module is cut-out to be replaced by more smaller modules, the necessary switchings will be requested simultaneously. However, the switchings are not necessarily performed simultaneously, as the exact time for switching is selected to minimize the transients as already explained.

The control strategy is constant cosφ control. The cosφ setpoint can be set on the local display or by remote control. Cosφ can be selected in the interval –1..1. For the first test period, a Mita-Teknik WP3000 controller has been used as central controller. The WP3000 is able to operate with a control times down to 70 ms, but to control faster than 100 ms would require a major revision of the software. To complete the test, the operation for faster control times was also investigated. For that purpose, the WP3000 controller was replaced by a Mita-Teknik IC1000 controller, which is capable to down to 40 ms without software modifications.

The measurement module in the central Mita-Teknik unit controller is connected to its own voltage transducers and current transformers, which are mounted on the busbars in the switchboard of the Nordtank wind turbine. Moreover, the start/stop signal from the wind turbine control system, is used by the central Mita-Teknik unit controller.

3 Test

3.1 Test setup

3.1.1 Grid connection

The unit is tested on the 500 kW Nordtank wind turbine in Risø. The connection diagram is shown in Figure 1.

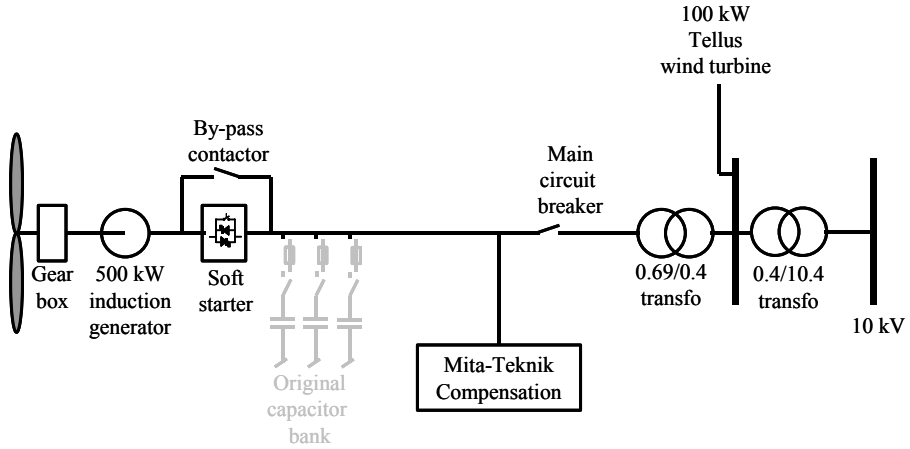

Figure 1: Connection diagram of Mita-Teknik compensation to 500 kW Nordtank in Risø

The Nordtank wind turbine is connected to a 400 V grid, designed for test of smaller wind turbines. Thus, the 1000 kVA, 0.4 / 10.4 kV transformer is presently shared between the 500 kW Nordtank wind turbine and a 100 kW Tellus wind turbine.

The Nordtank wind turbine is rated 690 V, and therefore an additional 800 kVA, 0.69 / 0.4 kV transformer is installed to step down the voltage of the wind turbine to the 400 V grid.

The original capacitors, which are normally switched with contactors, are disconnected during the test, simply by removing the fuses as illustrated in Figure 1.

3.1.2 Measurement points

The measurement points for the compensator and Risøs measurements are on the busbar in the wind turbine 690 V board. The exact positions of the measurement points relative to the compensator are illustrated in Figure 2.

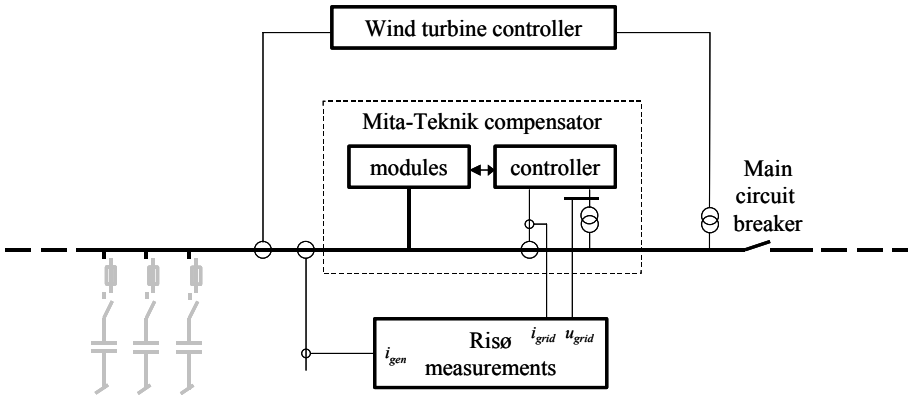

Figure 2: Measurement points

There is only one relevant voltage measurement point. The wind turbine controller has its own 3 phase voltage transformers, while the Mita-Teknik has installed dedicated 3 phase voltage transformers (400 / 18 V) for the Mita-Teknik controller. The Risøs measurement system uses Mita-Tekniks voltage transformers to measure the grid voltage

There are two different current measurement points, one on the generator side and one on the grid side of the Mita-Teknik compensator. The wind turbine control system measures on the generator side using its own current transformers. The Mita-Teknik compensator measures with 800 / 1 A current transformers on the grid side, as it performs a close loop control of the reactive power to the grid.

Risøs measurement system shares the Mita-Teknik current transformers on the grid side, and in addition to that measures with its own 500 / 1 A current transformers on the generator side. The idea is that the reactive power fluctuations on the generator side will correspond quite well to the reactive power fluctuations if the wind turbine runs with the original contactor switched compensation, only the mean value of the reactive power will change if the original capacitors were used.

3.1.3 Risø measurement system

Since the secondary voltage of the voltage transformers is rated ± 18 V_{RMS}, and Risøs measurement system has maximum range ± 5V_p, three Tektronix P5200 High Voltage Differential Probes are used to measure on the secondary side of the voltage transformers with 50/1 ratio. The 3 dB bandwidth of the Tektronix P5200 probes is from DC to 25 MHz, so the bandwidth is of the combined measurement is probably limited by the voltage transformers, for which we do not know the bandwidth. However, for the present measurements, the bandwidth is assumed to be sufficient. All 3 phases of line-to-neutral voltages are measured.

Since the current transformers provide currents on the secondary sides, and Risøs measurement system requires voltage inputs, the secondary currents are measured with flexible LEM-flex RR 3000-SD/48 AC current probes with a 3 dB bandwidth from 8 Hz to 100 kHz and a 100 mV/A gain.

Risøs data acquisition is illustrated in Figure 3. It consists of a laptop equipped with an analogue to digital converter (ADC) dedicated fast measurements of instantaneous voltages and currents. The ADC gets its analogue input signals through a signal conditioning equipment providing filtering, amplifica-

tion of the external input signals to the input range of the ADC, and simultaneous sampling of the filtered an amplified signals.

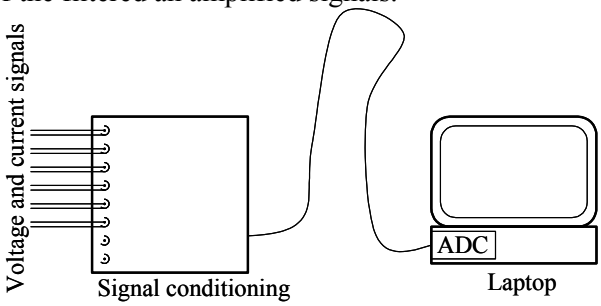

Figure 3. The data acquisition system

The laptop is a 1 GHz IBM ThinkPad with 128 MB RAM and a 28.6 GB HD.

The ACD card is a AI-16E-4 from National Instruments. The maximum sampling rate is 500 kS/s. The ADC card is inserted directly in the PCM-CIA slot of the laptop.

The signal conditioning unit is joined in the National Instrument SCXI-1000 chassis with 4 slots for SCXI cards. Only 2 slots are used in the present system.

The voltage and current sensor signals are connected through a SCXI-1305 BNC terminal block, in the ranges $\leq \pm 5$ V.

The terminal block is connected to the front of a SCXI-1141 8 channel elliptic lowpass filter block, which occupies the first slot in the SCXI-1000 chassis. The SCXI-1141 is equipped with programmable cut-off frequency and programmable individual gains of the channels. The cut-off frequency of the filters can be programmed to frequencies from 10 Hz to 25 kHz, with available values f_c = 100 kHz / n where n is an integer. The individual channel gain makes it possible to adapt the voltage level of the input signals to the ±5V of the ADC and thus minimise the noise of the ADC. The maximum gain is 100, i.e full range of the ADC can be obtained with ±50 mV input signal, corresponding to 100 mV / 2^{12} = 24 μV step size. This filter gain feature is important in the present measurements, because the input signals to the signal conditioning are relatively small.

The SCXI-1141 filter block is then connected to a SCXI-1140 8 channel simultaneous sampling 8 channel differential amplifier block, which occupies the second slot in the SCXI-1000 chassis. The simultaneous sampling block sends the multiplexed signals via the SCXI bus to the first channel in the ADC in the laptop.

Risøs LQ software developed in Labview controls the measurement hardware and acquires the data to the harddisk of the Laptop. The sampling frequency of the ADC is set to 1 kHz, and the cut-off frequency 400 Hz for the long-term test consisting of 10 minute time series. The initial test described in 4 is performed with 10 kHz sampling frequency and 4 kHz cut-off frequency.

4 Test results

4.1 Initial unit test

Before the long-term test was initiated, the individual capacitor steps in the compensation unit were tested 20 November 2003, applying the control panel of the unit when the wind turbine was stopped.

Figure 4 shows active and reactive power during the initial test. As can be confirmed by the reactive power, the units were tested one after the other, in the sequence 1 (2.5 kvar), 2 (5 kvar), 3 (10 kvar), 4 (20 kvar), 5 (40 kvar), 6 (80 kvar), 7 (80 kvar) and 8 (80 kvar).

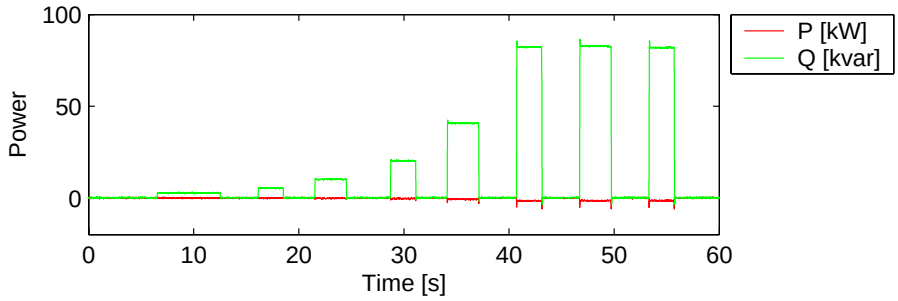

Figure 4: Active and reactive power during the 60 seconds initial test

It also appears from Figure 4 that the losses increase with the step size. The green curve (reactive power) is approximately zero when no module is connected, and it can be seen that the active power is below that when the large modules are connected, while the active power is very close to zero when the small modules are connected.

The measured losses are 1.5 kW for the 80 kvar step, but the active power measurement is very uncertain in this case, because it is very sensitive to small phase errors in voltage-current measurements. Thus 0.5 deg phase error will cause 700 W measurement error in active power, because of 80 kvar reactive power.

The main contribution to the losses are expected to be the voltage drops over the thyristors which has be calculated to 180 W totally for all three phases in a 80 kvar step. In addition to that, the losses in capacitors should be 0.5 W/kvar, i.e. 40 W for a 80 kvar step. The discharge resistors contribute to the losses with only 7 W totally in the 80 kvar step.

Figure 5 shows the 3 phase currents for connection of the first 80 kvar step (step 6). The capacitors are completely discharged when they are connected, so the connection will take place at the zero crossing of the voltages, which is confirmed in Figure 6.

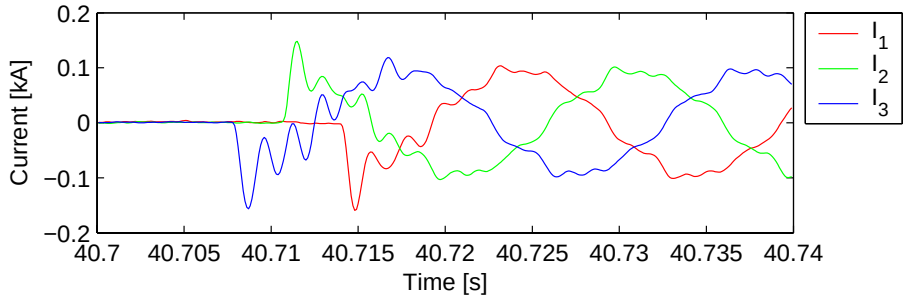

Figure 5:Currents for connection of (completely discharged) 80 kvar step with stopped wind turbine

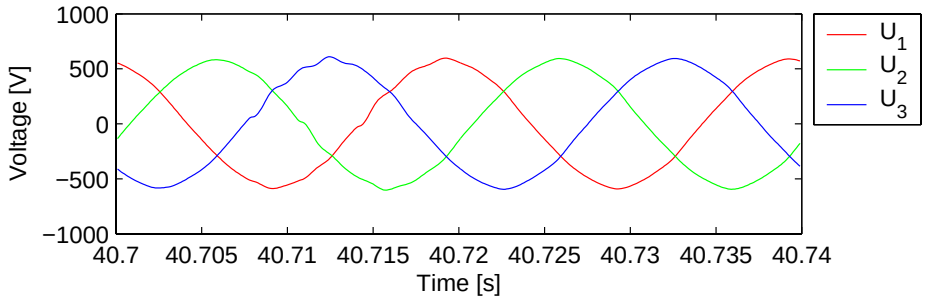

Figure 6: Grid voltages for connection of (completely discharged) 80 kvar step with stopped wind turbine

The steady-state current is 90 deg phase displaced from a steady state voltage. In this case the current is behind the voltage, because production sign is used in the measurements. Because of the 90 deg displacement, the steady state current is at the peak (maximum or minimum) when the voltage crosses zero. Therefore, the currents will try to step to maximum or minimum immediately after connection at zero voltage. However, the currents are supplied through the transformer(s), and therefore it cannot step discontinuously. Instead, the resonance between transformer leakage reactances (plus 10 kV grid reactance) and the capacitor is excited, resulting in a resonance oscillation as seen in Figure 5, with the resonance frequency f determined as

$$f = \frac{1}{2\pi\sqrt{LC}} \tag{1}$$

where L is the inductance and C is the capacitance.

Figure 7 show the 3 phase currents for another connection of the first 80 kvar step (step 6). This time, the capacitors are charged, but not to the peak grid voltage, as they were switched off only 3 seconds earlier (at time 8 s). In this case, the connection takes place right before the maximum (or minimum) voltage is reached, which is confirmed by the voltages in Figure 8.

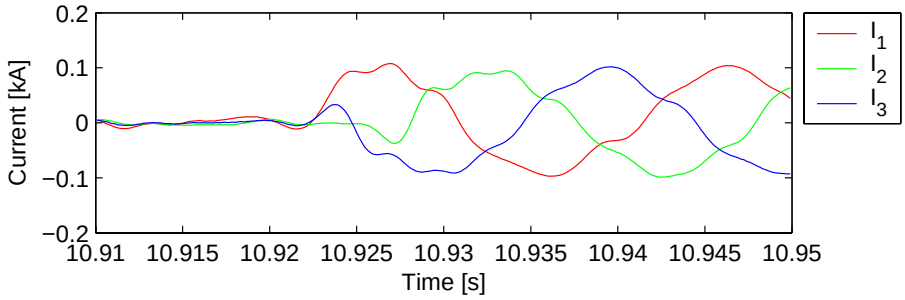

Figure 7:Currents for connection of charged 80 kvar step with stopped wind turbine

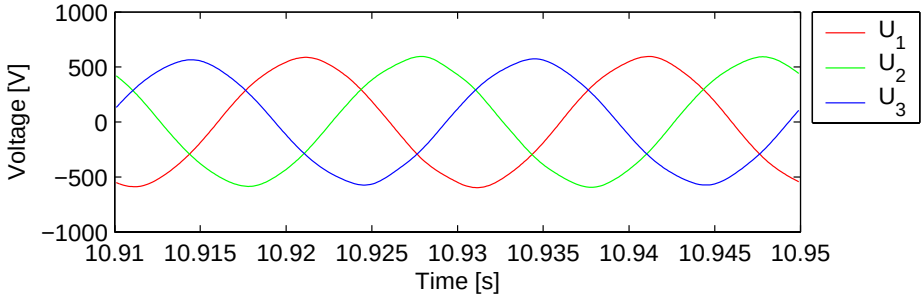

Figure 8: Voltages for connection of charged 80 kvar step with stopped wind turbine

Comparing Figure 5 and Figure 6 to Figure 7 and Figure 8, it becomes clear that the switchings of charged capacitors remove the transient overcurrents, which are present for switching of discharged capacitors. This is because the capacitors are switched on at a time where the derived voltage is approximately zero, i.e. the charging current is zero before and after the switching. Consequently, both voltages and currents are without steps, and the transients are practically zero.

For comparison, the voltages and currents for connection of one of the 50 kvar capacitor steps in the original Nordtank capacitor bank with the original contactors are shown in Figure 9 and Figure 10. It is clear that the current and particularly the voltage transients are significantly reduced with the Mita-Teknik compensator. This is because the synchronisation of the thyristor closing to the time where the grid voltage is equal to the capacitor voltage is very successful.

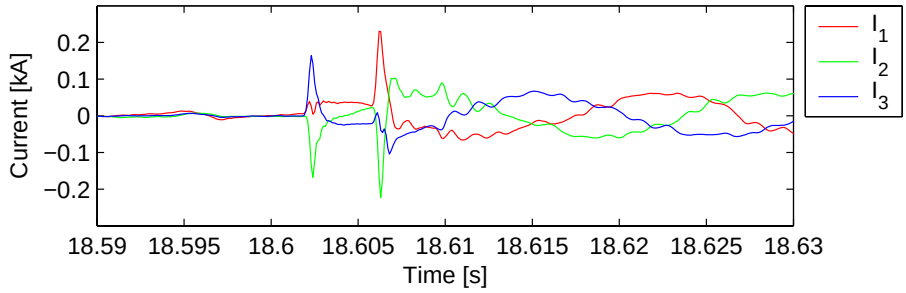

Figure 9: Currents for connection of (completely discharged) 50 kvar step with conventional contactor and stopped wind turbine

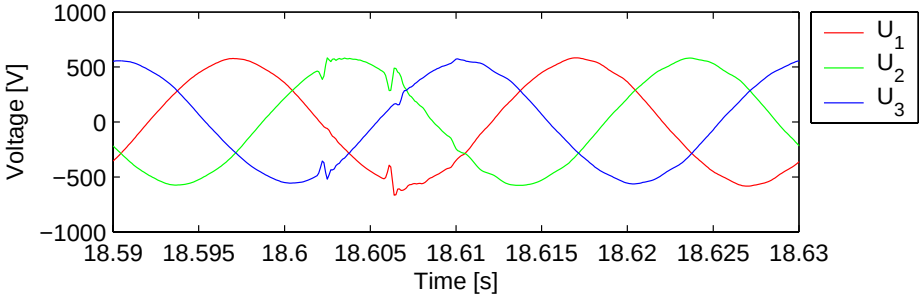

Figure 10: Voltages for connection of (completely discharged) 50 kvar step with conventional contactor and stopped wind turbine

Figure 11 shows the currents at the connection of the 20 kvar step. It is seen that the oscillation frequency is doubled compared to Figure 5, which is as expected from (1) because the capacitance now is 4 times smaller.

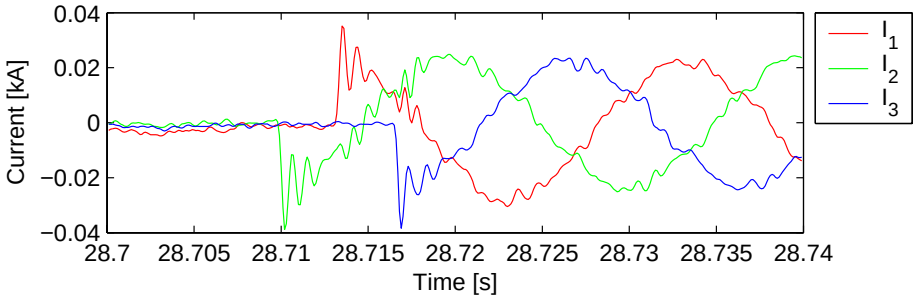

Figure 11: Currents for connection of (completely discharged) 20 kvar step and stopped wind turbine

Finally, the currents and voltages for disconnection of the 80 kvar step is shown in Figure 12 and Figure 13. It is seen that the disconnection very successfully takes place at the zero crossing of the currents and that there are no transients in voltages or currents.

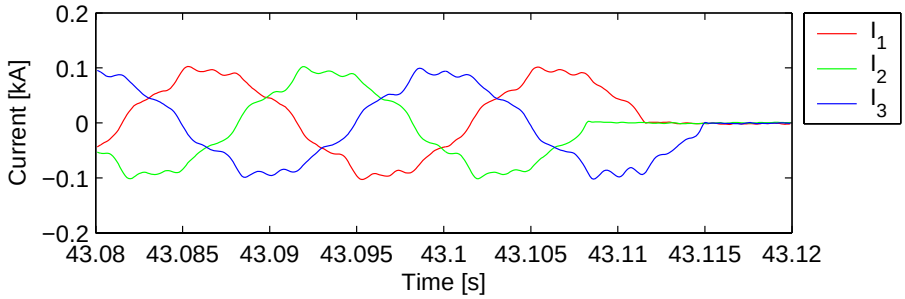

Figure 12: Currents for disconnection of 80 kvar step with stopped wind turbine

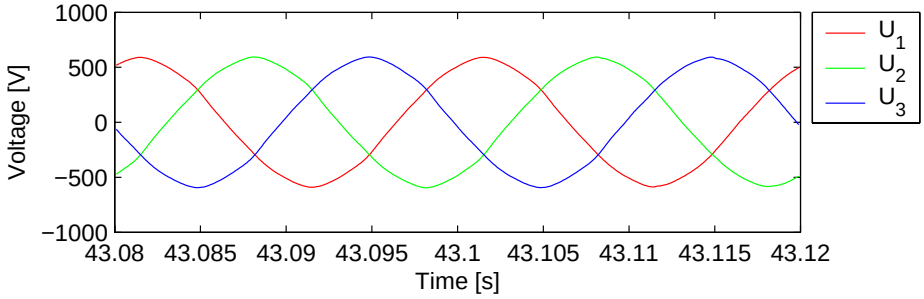

Figure 13: Voltages for disconnection of 80 kvar step with stopped wind turbine

To conclude at this stage, the switching transients are significantly reduced compared to switching with the conventional mechanical contactors, because the switching in takes place when the capacitor voltage is equal to the grid voltage, while the switching out takes place when the current is zero.

However, there are some transients in the switching in of completely discharged capacitors, because the capacitor currents would step to maximum when they are switched in immediately after a zero crossing of the voltage. However, it is not possible for the current to step because it should be delivered from the transformer, and a current step in the transformer would cause infinite voltage. The result is an oscillation with the frequency according to (1), where C is the capacitance of the step and L is the inductance of the connecting grid. If the grid has a high resistance, then that would damp the oscillation. Consequently, the oscillation frequency and damping highly depends on the grid. This grid dependence of the oscillation also explains why the early test of the unit in Mita-Tekniks laboratory showed much less transients than what was measured on the wind turbine in Risø.

If the capacitors are charged to the peak value of the voltage, then the switching in transients are removed, because the switching then takes place when the derived voltage is zero, i.e. the switching does not cause a current step in the capacitor.

Concerning the disconnection, it is practically free of transient oscillations.

The transients measured in the present section have all been measured with disconnected wind turbine. It is expected to have an influence on the transients when the wind turbine is connected, but in that there is much more distortion, and therefore, it is more difficult to extract the switching transients.

4.2 Long term test statistical results

4.2.1 General

The long term measurements have taken place with some interruptions in the period 29 November – 15 December 2003. In that period, the unit was tested with different sample times T_{sc} in the controller, and different power factors $\cos\varphi$.

We will present results from two periods. The first period (29 November – 1 December) the compensation unit was set to run with T_{sc} = 300 ms and $\cos\varphi$ = 0.99. In that period, the power ranged from 0 to 420 kW, corresponding to a wind speed range from 3 to 11 m/s. Most of the time, the wind speed was above cut-in, and the turbine ran without problems, resulting in 225 ten-minute runs at continuous operation of the wind turbine, i.e. continuously active compensation unit.

The second period (11 – 15 December) the compensation unit was set to run with T_{sc} = 100 ms and $\cos\varphi$ = 1.00. In that period, the power ranged from 0 to 534 kW, corresponding to a wind speed range from 3 to 16 m/s. However, because the wind turbine stopped due to a fault over the weekend, only 171 ten-minute runs at continuous operation of the wind turbine are available for that period.

4.2.2 Steady state reactive power and power factor

Figure 14 shows measured ten minute averages of reactive power Q on the grid side, vs active power P for the first selected period, i.e. with $\cos\varphi$ = 0.99. For comparison, the exact cosφ=0.99 line is also shown.

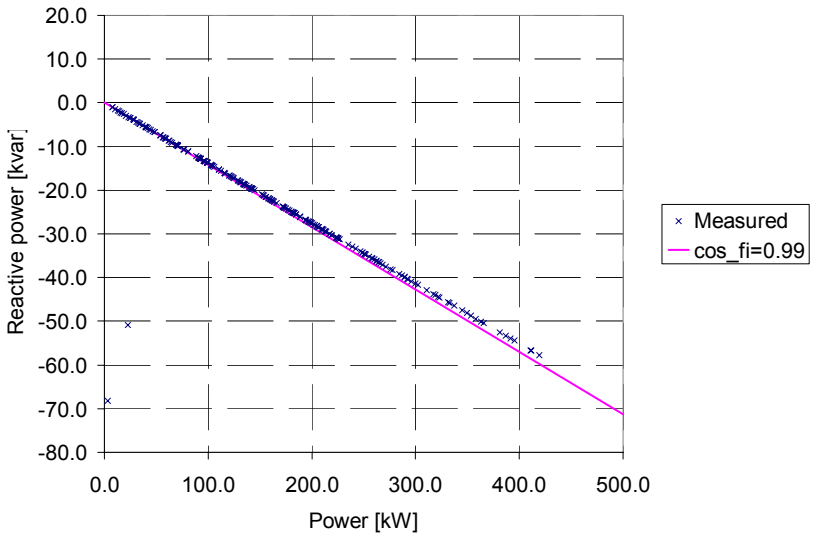

Figure 14: Measured ten minute averages of Q(P) for Mita-Teknik compensated wind turbine with cosφ=0.99 compared to exact cosφ=0.99

Figure 15 shows the compensated reactive power from Figure 14 together with the reactive power measured on the generator, and the corresponding reactive power if the wind turbine had run with its original no-load compensation. The latter values are simply found by adding the rated reactive power of the no-load compensation (corrected for the influence of the voltage deviation from rated voltage) to the measured reactive power of the generator.

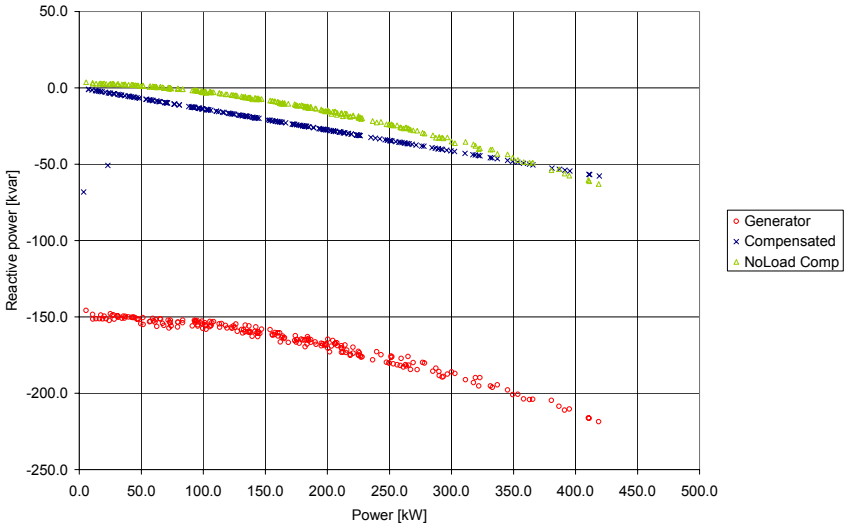

Figure 15: Measured ten minute averages of Q(P) for Mita-Teknik compensated wind turbine with cosφ=0.99 compared to measured generator reactive power and expected reactive power with original no-load compensation.

Figure 16 shows measured ten minute averages of reactive power *Q* on the grid side, vs active power *P* for the second selected period, i.e. with cosφ = 1.00. For comparison, the exact cosφ=1.00 line is also shown.

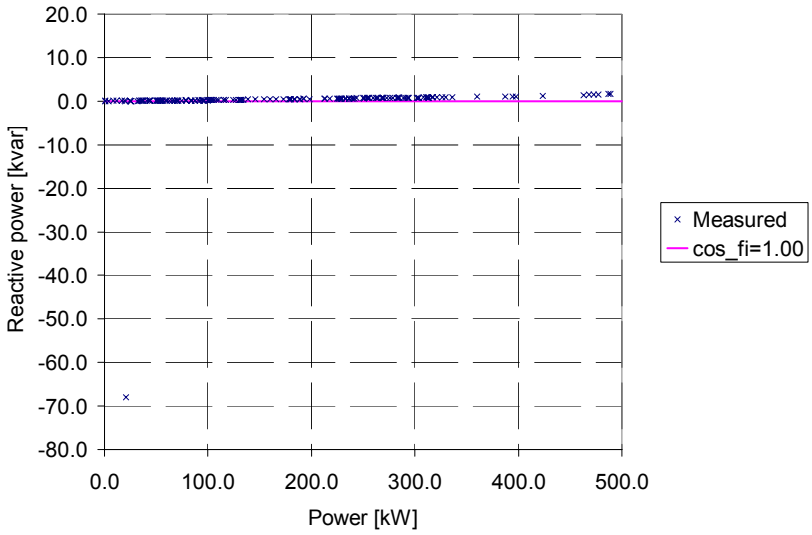

Figure 16: Measured ten minute averages of Q(P) for Mita-Teknik compensated wind turbine with cosφ=1.00 compared to exact cosφ=1.00

Figure 14 and Figure 16 first of all show that the compensation works fine in steady state. The reactive power points are on a line quite close to the setpoints of cosφ. The deviation, approximately 1 kvar pr. 350 kW, corresponds to 0.16 deg phase error in the measurement. Moreover, the measured reactive power is production, but the actual control is set to always consume a little reactive power from the grid. Still, it is a very small error, which could in principle be in the Risø currents clamps or in the Mita-Teknik compensator.

4.2.3 Flicker emission

According to IEC 61400-21 [1], the flicker coefficient should be measured for different grid impedance angles 30 deg, 50 deg, 70 deg and 85 deg. Ideal dynamic control of the power factor elimination of flicker for a given grid impedance angle. This can be seen as follows:

In IEC 61400-21, the grid is simplified to an ideal source in series with a resistance R and a reactance X. This simplification is often applied, and it corresponds to the data on short circuit power, which is normally available from the grid operator. In this case, the grid impedance angle ψ is determined by the X/R ratio according to

$$\tan\psi = \frac{X}{R} \tag{2}$$

The dynamic changes ΔU in the voltage U can approximately be determined by

$$\frac{\Delta U}{U} \cong \frac{P \cdot R + Q \cdot X}{U^2} \tag{3}$$

Combining the power factor definition

$$\cos\varphi = \frac{P}{S} = \frac{P}{\sqrt{P^2 + Q^2}} \tag{4}$$

with (2) and (3), it can be shown that the voltage changes can be zero, i.e. $\Delta U = 0$, with a leading (P>0 $\Rightarrow$ Q<0) power factor $\cos\varphi = \sin\psi$. Since flicker is a measure for voltage changes, zero voltage change corresponds to zero flicker, so flicker can ideally be eliminated if $\cos\varphi = \sin\psi$.

Table 1 shows the ideal power factor $\cos\varphi$ for elimination of flicker on grid with impedance angle ψ. Obviously, the grid operator would normally not accept $\cos\varphi = 0.5$ to eliminate flicker, because the reactive power consumption would cause other problems such as increased losses and voltage stability problems.

Table 1. Ideal power factor $\cos\varphi$ for elimination of flicker on grid with impedance angle ψ.

ψ [deg]	30	50	70	85
$\cos\varphi$	0.500	0.766	0.940	0.996

It is indicated from the numbers in Table 1 that with $\psi = 85$ deg, high power factors as 0.99 and 1.00 should be expected to reduce flicker. It can also be shown that a power factor of 0.99 will ideally remove flicker from a grid with impedance angle 81.9 deg, like a power factor of 1.00 ideally remove flicker from a grid with impedance angle 90 deg. Therefore, the 85 deg flicker coefficients c_{85} is selected for the comparisons below.

Figure 17 shows 85 deg flicker coefficients c_{85} during the first selected measurement period, i.e. with $T_{sc} = 300$ ms and $\cos\varphi = 0.99$. It is seen that the flicker coefficients are higher in the compensated (wind tubine) point than in the uncompensated (generator) point. The 99 % percentile, which should be reported according to IEC 61400-21, is not determined, but a qualified guess would be 2-2.5 for the uncompensated and 3-3.5 for the compensated, i.e. approximately 50 % higher flicker coefficient with compensation.

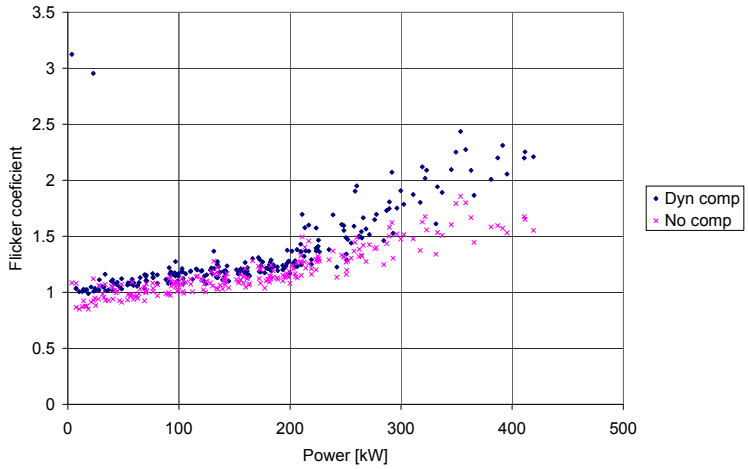

Figure 17: Measured flicker coefficients c_{85} of dynamically compensated and uncompensated currents for runs with controller sample time T_{sc}=300 ms and power factor $\cos\varphi$=0.99.

Figure 18 shows the same result during the second selected period, i.e. with $T_{sc} = 100$ ms $\cos\varphi = 1.00$. In this case, the flicker coefficients are less correlated

with the average power, which is because the wind directions have changed more, and the turbulence varies significantly with the wind direction.

It is seen that also in this case, the flicker coefficients are higher in the compensated (wind turbine) point than in the uncompensated (generator) point. The 99 % percentile can be estimated to approximately 3-3.5 for the compensated in this case as well, i.e. no improvement by increasing the controller sample time.

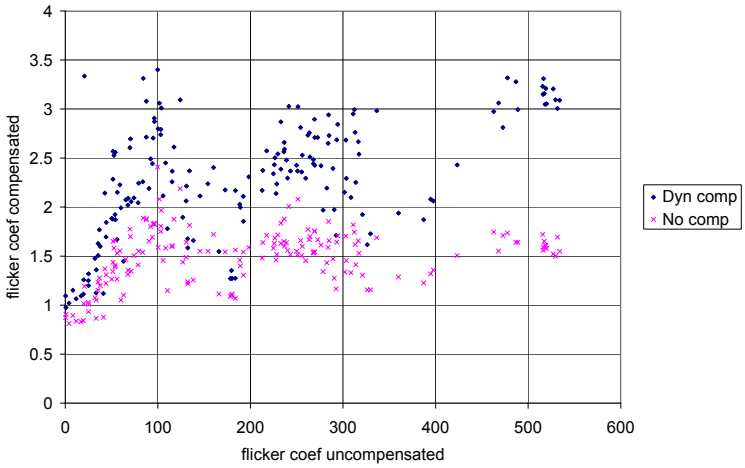

Figure 18: Flicker coefficients c_{85} of uncompensated and compensated currents for runs with controller sample time T_{sc}=100 ms and power factor cosφ=1.00.

As it is seen from section 4.3 below, the flicker emission with dynamic compensation has been reduced, but it has not been possible to come below the flicker emission without dynamic compensation. This will be discussed further in section 4.3.

4.3 Dynamical analyses

The purpose of this section is to get some more insight to why the flicker coefficients are not improved by the compensation unit. Some improvements are tested and shown, but still it has not been possible to get below the flicker emission without compensation.

First we will look at the operation during 10 seconds at high wind speed with T_{sc} = 300 ms and cosφ = 0.99. Figure 19 shows the power variation in the selected period.

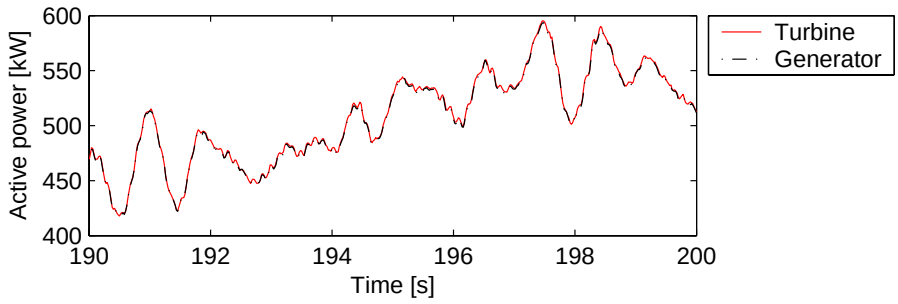

Figure 19: Power during selected 10 seconds at high wind.

If the power factor is kept constant, the reactive power can be determined by

$$Q = -P \cdot \sqrt{\frac{1}{(\cos\varphi)^2} - 1} \tag{5}$$

In Figure 20, the measured reactive power on the wind turbine terminal is compared to the ideal reactive power calculated with (5). It can be seen from the figure that the measured reactive power fluctuates much more than the ideal reactive power, and therefore the flicker emission can be higher with compensation than without.

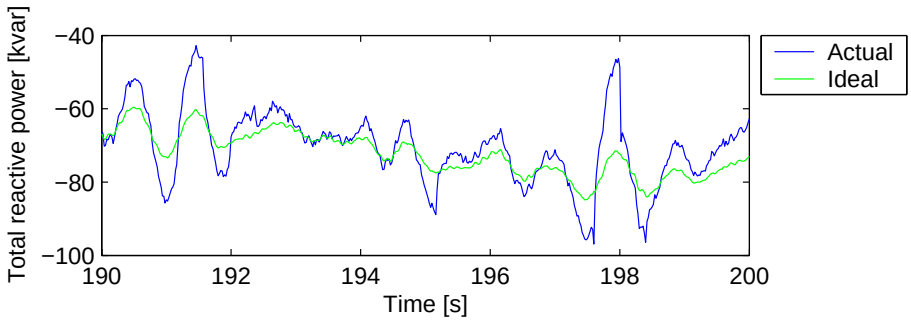

Figure 20: Actual and ideal reactive power at wind turbine terminal with compensator cosφ=0.99 and T_c=0.3 s.

The reason why the measured reactive power fluctuates much more than the ideal reactive power becomes clearer in Figure 21. The reactive power output from the compensation unit is compared to the ideal output, i.e. $Q_{comp} = Q - Q_{gen}$ using measured and ideal Q respectively, together with measured Q_{gen}. It can be seen from the figure that the compensation unit responds too slow, and the result is actually that the dynamic variations in the generator reactive power become worst by the attempt to control them out. Mita-Teknik also checked the software after this measurement, and found that the reactive power measured in the beginning of a 300 ms period is used to control reactive power in the end of the same 300 ms period, i.e. with 300 ms delay. This can also be seen as a delay in Figure 21, but it is a consequence of the sampled control.

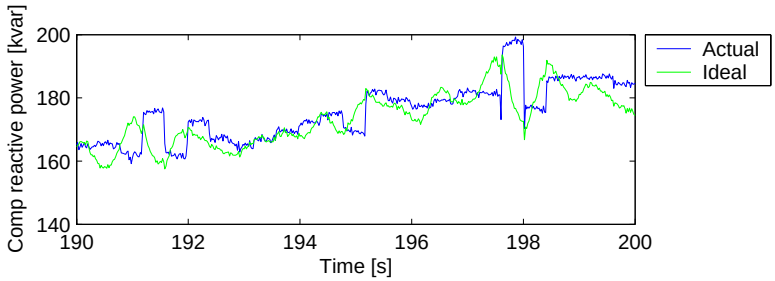

Figure 21: Actual and ideal reactive power of compensator unit terminal with compensator cosφ=0.99 and T_c=0.3 s.

The standard way to avoid such instability in the control is to apply a measurement filter, which filters the measurement before it is fed back too the controller. However, since instantaneous (fast varying) voltages and currents are used as input to calculate the reactive power, the controller should sample sufficiently fast to follow the curve form of the 50 Hz, calculate instantaneous reactive power from that and apply a digital filter on the calculated reactive power before it is fed back to the controller. The cut-of frequency of the digital filter should be maximum half of the fast sampling frequency to avoid aliasing.

The fluctuations in the power are due to a combination of the so-called 3p effects and mechanical and electrical eigenfrequencies, primarily in the drive train.

The 3p effect is caused by the rotation of the blades in a wind speed field which is not constant. An intuitive way to understand the 3p effect is to look at the tower shadow effect. Every time a blade passes the tower, the wind speed seen by the blade drops, and consequently the power drops. This happens with 3 times the rotational speed, i.e. with the 3p (3 periods) frequency. In the real world, the turbulence also contributes to the 3p effect, because the turbulence varies over the rotor area.

The important 3p frequency is in this case (with rotor speed 27 rpm) 1.35 Hz. Figure 22 shows the PSD (power spectral density) of the power, and the 3p frequency can be identified, although is some cases it is more pronounced.

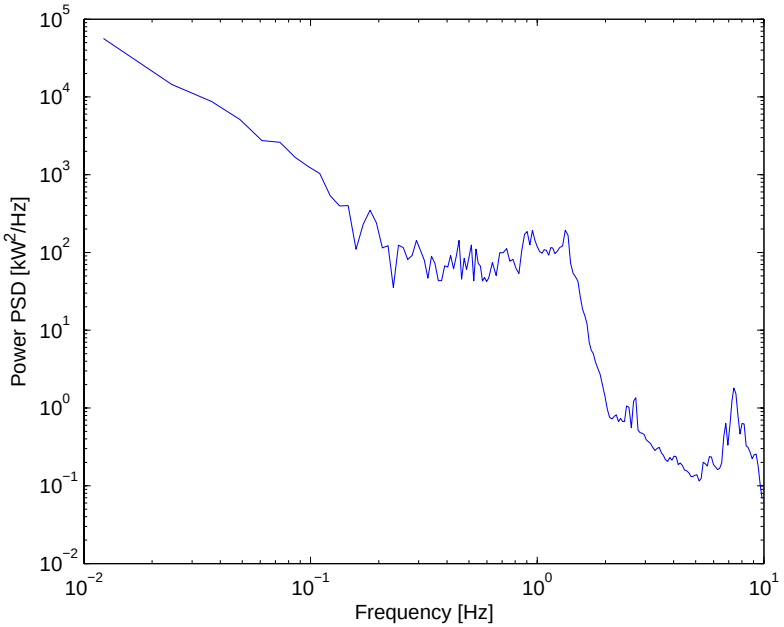

Figure 22: PSD of wind turbine power.

It has earlier been shown that the 3p effect is responsible for most of the flicker emission during continuous operation of wind turbines with fixed speed(s) [2],[3]. Since the rotor speed, and consequently the 3p frequency, typically decreases with increased rated power of wind turbines, the required sampling frequency for the compensation unit to be able to reduce flicker will typically be less for larger wind turbines.

On this background, it should be expected that the flicker emission could be reduced with a higher sampling frequency, but that was not the case as it was seen from Figure 18. Figure 23 shows the measured reactive power from the

compensator compared to the ideal for a case where cosφ=1.00 and T_{sc} = 100 ms. It looks like the compensator is actually responding slower than the 100 ms. A reasonable explanation is that the switchings are delayed because the voltages on the capacitors are not enough discharged to be equal to the grid voltage peak. This can happen because when the capacitor is switched off, the grid voltage steps down, so it becomes less than the capacitor voltage.

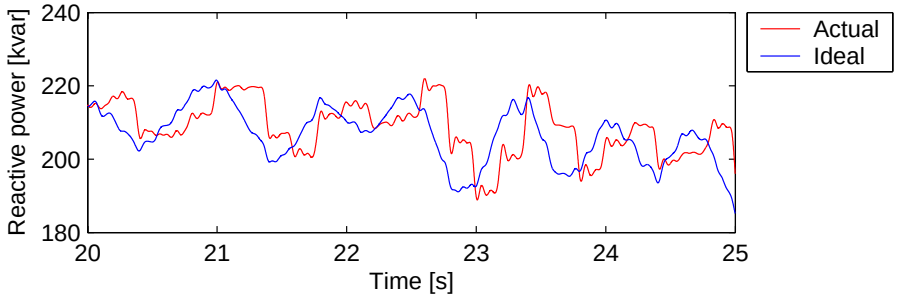

Figure 23: Actual and ideal reactive power from compensator, with cosφ=1.00 and T_{sc}=100 ms.

Figure 24 shows the PSDs of reactive power from compensated wind turbine compared to the reactive power of the generator only. The PSD confirms that the 3p contribution around 1.35 Hz is not reduced, which is also indicated in Figure 23, where it looks like the 3p gets a phase displacement rather than a reduction. Moreover, Figure 24 shows that the compensator adds energy above the 3p frequency, which is the reason for the higher flicker with compensation.

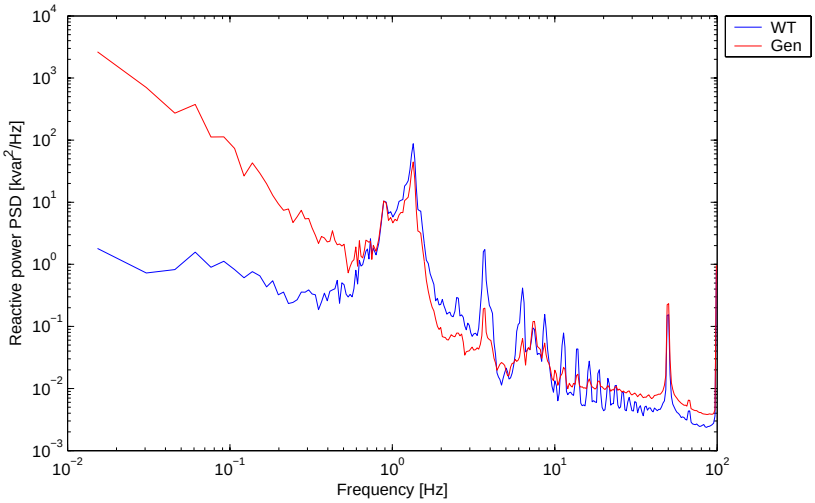

Figure 24: PSD of reactive power from compensated wind turbine (WT) compared to the reactive power of the generator only (Gen), with cosφ=1.00 and T_{sc}=100 ms.

This is confirmed in Figure 25, where the flicker coefficients are calculated based on active and reactive power instead of currents and voltages. The power

based flicker calculation is not according to the IEC 61400-21 specifications, but it gives results close to the specified current / voltage procedure. The reason to use power based flicker in Figure 25 is that it makes it possible to filter the power before flicker is calculated, and that way it is possible to identify which frequencies contribute most to flicker. The filter applied to active and reactive power is a 6th order Butterworth low-pass filter, and the figure shows the flicker coefficient vs. the cut-off frequency. It is seen that the additional flicker with the compensation comes from noise at the 3p frequency and above, where the flicker sensitivity is known to be very high. The noise above the 3p frequency is most likely due to the step changes in reactive power due to the switching of capacitors.

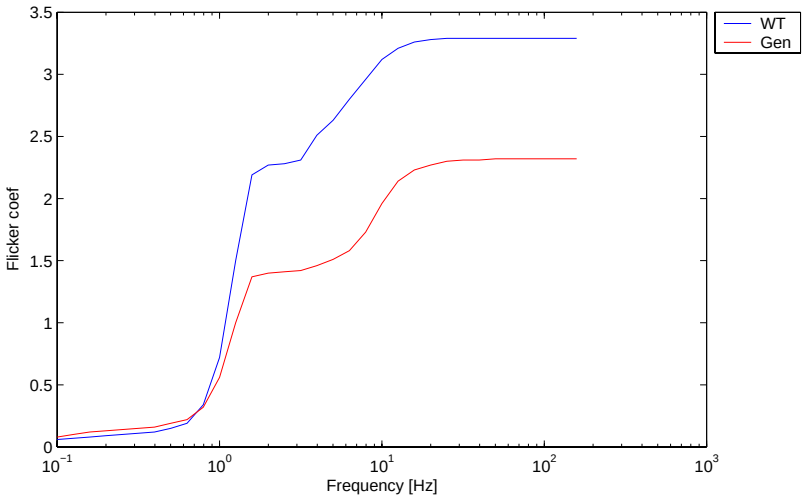

Figure 25: Flicker coefficients calculated with filtered active and reactive power shown vs. filter cut-off frequency, for compensated wind turbine (WT) compared to the reactive power of the generator only (Gen), with cosφ=1.00 and T_{sc}=100 ms.

The additional flicker due to reactive power steps cannot be completely avoided, but it becomes worst because the step sizes are high. The high step sizes are a consequence of the control strategy and the hardware, which could not shift faster than with 200 – 300 ms, even though the sampling step size T_{sc}=100 ms. First of all, this is because the capacitors are discharged too slowly after they are disconnected as mentioned above. Another problem is that 100 ms is too slow to have a significant reduction in flicker, and also implies that the capacitor steps are relatively high. However, the Mita-Teknik WP3000 controller cannot control faster than 70 ms, and to make it control faster than 100 ms, the software should be modified significantly.

As a consequence of these hardware problems, the Mita-Teknik WP3000 controller was replaced by a Mita-Teknik IC1000 controller, which is able to sample with T_{sc}=40 ms. Moreover, additional discharge resistances were mounted, which increased the discharge constant of the capacitors.

Figure 26 shows the PSDs of 10 minutes time series of measurements with the replaced controller running with T_{sc}=40ms. Comparing to Figure 24 it is observed that the 3p frequency is now successfully rejected. Actually the PSDs cross at 2 Hz, which means that the converter can compensate for reactive power fluctuations up to 2 Hz.

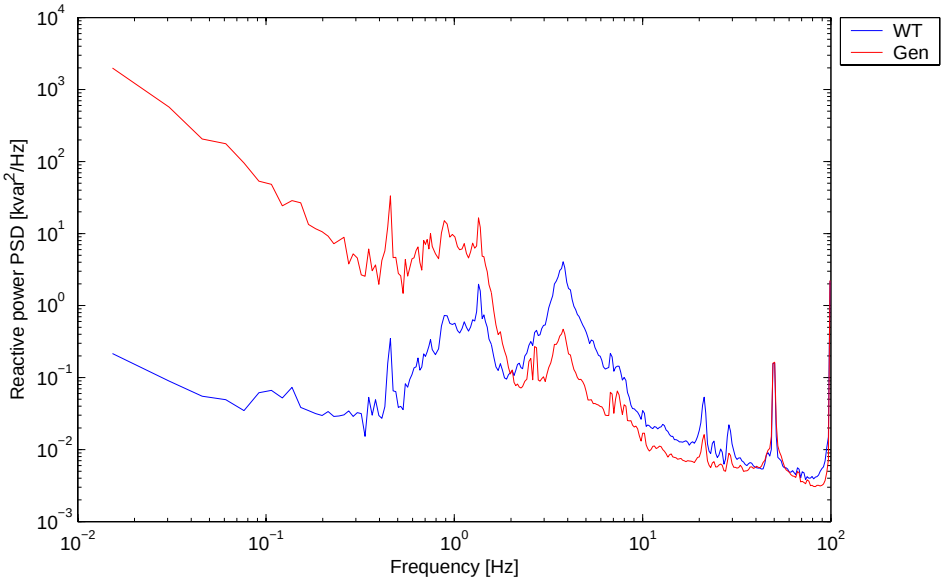

Figure 26: PSD of reactive power from compensated wind turbine (WT) compared to the reactive power of the generator only (Gen), with Mita-Teknik IC1000 controller, cosφ=1.00 and T_{sc}=40 ms.

However, it is also noticed that there is a significant top at 3.8 Hz in the compensated (WT) PSD as well as the uncompensated (Gen) PSD. The window of the time series in Figure 27 show an example of what happens several times every minute: The converter seems to operate properly, but then it suddenly makes a number of large steps like an oscillation. This could be due to a software error in the control, and it will be looked into by Mita-Teknik.

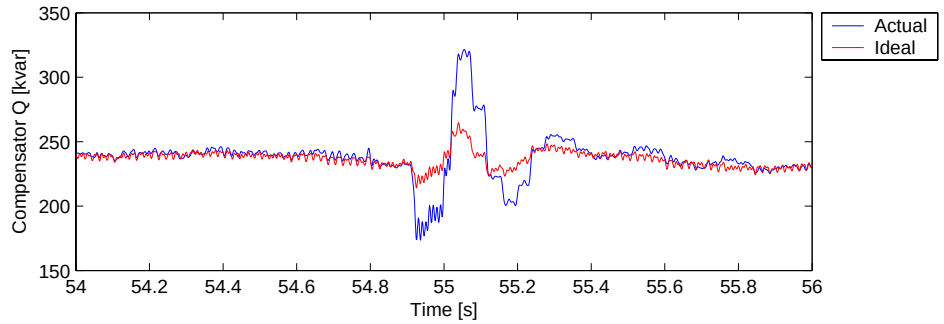

Figure 27: Actual and ideal reactive power of compensator, with Mita-Teknik IC1000 controller, cosφ=1.00 and T_{sc}=40 ms.

It is noticed that the ideal reactive power also steps as a consequence of the compensator steps, because the generator reactive power steps when the generator voltage changes. So the assumption that we measure the wind turbine as it would have operated without compensation is not quite true. It is also seen that

the 3.8 Hz top is also visible on the PSD of the generator reactive power in Figure 26.

Figure 28 shows the flicker coefficients of the filtered active and reactive power. It is seen that the flicker level due to the 3.8 Hz is very high, and also that it influences the compensated wind turbine flicker emission as well as the flicker emission from the generator alone as indicated in Figure 27.

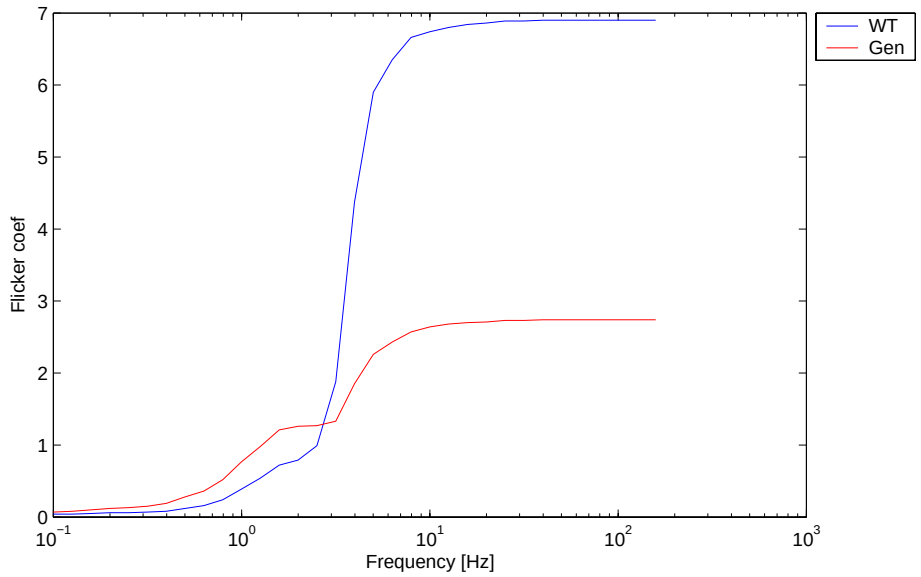

Figure 28: Flicker coefficients calculated with filtered active and reactive power shown vs. filter cut-off frequency, for compensated wind turbine (WT) compared to the reactive power of the generator only (Gen), with Mita-Teknik IC1000 controller, cosφ=1.00 and T_{sc}=40 ms.

Further detailed study of the 3.8 Hz oscillations have suggested that it is caused by a conflict in the control: If the controller requests a step to connect, it is attempting to do so, and when all 3 phases are connected, it returns ok status back to the controller. The oscillations take place when only one or two phases are ready, and therefore status is “not ready“. The controller therefore disconnects the step assuming that it does not work. But because it already is compensating partly, the reactive power steps down. This happens quite often because the controller sample time has become very low

The control strategy was then modified by Mita-Teknik, and the resulting operation is documented in Figure 29 and Figure 30. It is seen that the flicker due to reactive power steps are reduced, but some of the 3.8 Hz fluctuations are left, and flicker emission is still lower without compensation.

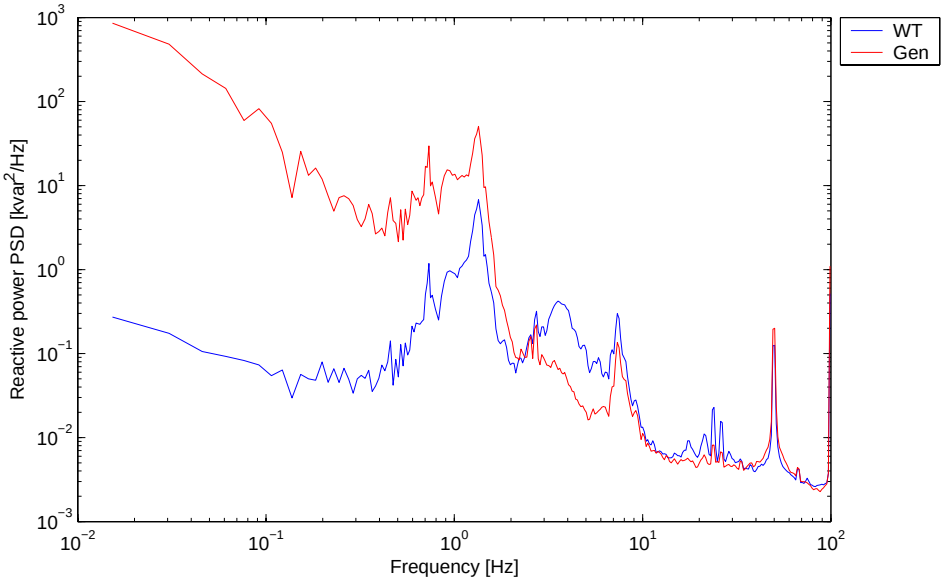

Figure 29: PSD of reactive power from compensated wind turbine (WT) compared to the reactive power of the generator only (Gen), with Mita-Teknik IC1000 controller, modified software, cosφ=1.00 and T_{sc}=40 ms.

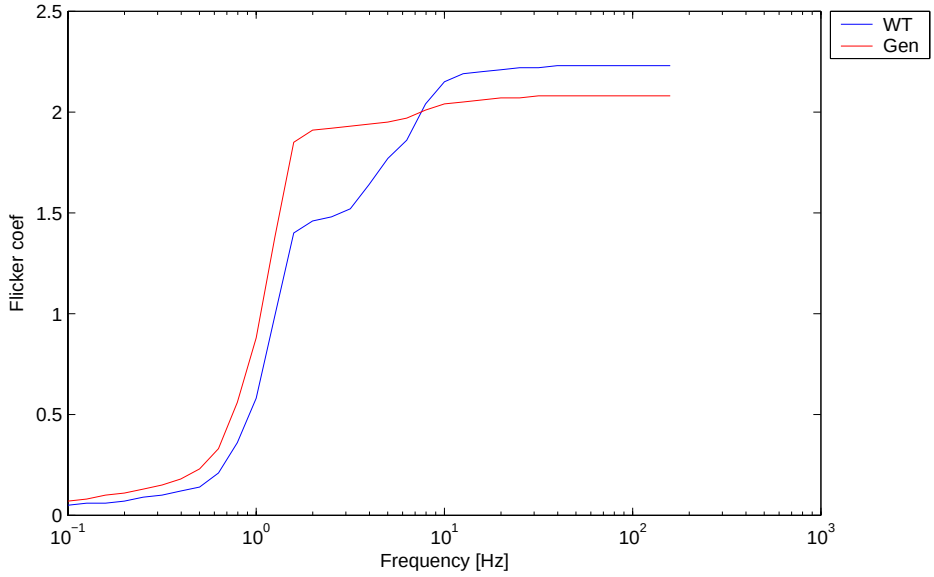

Figure 30: Flicker coefficients calculated with filtered active and reactive power shown vs. filter cut-off frequency, for compensated wind turbine (WT) compared to the reactive power of the generator only (Gen), with Mita-Teknik IC1000 controller, modified software, cosφ=1.00 and T_{sc}=40 ms.

The conclusion on the dynamic analyses is that with the applied control strategy, it has not been possible to reduce the flicker emission. But on the other hand, the increase in flicker should be minimised. This can also be obtained if the control is slowed down instead of speeded up. If the control is slowed down, the steps will be less frequent and consequently cause less flicker emission.

It is also recommended to filter the reactive power measurement for the controller, which is currently controlling on the instantaneous value of reactive power.

4.4 Capacitance change test

In order to quantify any changes in the capacitances in the compensation unit, a test similar to the initial test (performed 20 October 2003) reported in section 4.1 was performed 27 February 2004, i.e. after 4 months of operation with very fast switching frequencies.

For both tests, the admittances in all three phases were first calculated using Risøs power quality software. The software is first used to fit amplitude and phase of the fundamental components of currents and voltages. Then the fundamental voltages and currents are used to determine the admittances in the 3 phases as time series. Then the periods (each 2 seconds) where the individual steps have been connected are used to find average admittances. To correct for the stand-by admittance, the average admittances of each phase are also found in a periods (4 seconds in both tests) without any steps connected. Finally, based on the two tests, the change in capacitance has been estimated. The results are shown in Table 2.

Table 2. Estimated changes in capacitances after 4 months of operation with fast switching frequency.

Step #	Rated capacitance [kvar]	Change Phase 1 [%]	Change Phase 2 [%]	Change Phase 3 [%]
1	2.5	2.52	-2.13	1.08
2	5	0.87	-1.92	0.19
3	10	-1.72	-1.44	-0.55
4	20	-1.09	-1.11	-1.15
5	40	-1.20	-1.22	-1.31
6	80	-0.55	-0.25	-0.80
7	80	-1.59	-1.04	-26.56
8	80	-1.29	-1.05	-1.61

First of all, it is noticed that phase 3 of step 7 has lost approximately ¼ of the original capacitance. This indicates that one of 4 capacitances is not working.

Secondly, it is seen as a tendency the capacitances have lost approximately 1% of their values. The only exceptions are for the two small steps, where the uncertainty in the admittance estimation is the highest. Loss of capacitance is an indication of lifetime consumption for the capacitors. However, the significance of estimated changes has not been studied.

5 Simulation models

5.1 General

Two simulation models have been built in Matlab/Simulink. The main model covers the system from wind to grid, including wind model, aerodynamical model, drive train elasticity, generator dynamics, compensation unit and grid. The second model simulates a flickermeter.

The wind-to-grid simulation model is based on the models developed in Matlab/Simulink af Aalborg University as a part of the Simulation platform project, Iov et all [4]. These models also include the wind model implemented by Langreder [5] for Risø National Laboratory.

In the present project, data for the Nordtank wind turbine including grid connection have been collected and inserted in the models, a transient model for thyristor swithing of capacitors has been developed, and a control model is implemented to demonstrate the operation with dynamic phase compensation, i.e. fast reactive power control. Moreover, some adjustments of the Simulation Platform model has been done to reduce the simulation time. Finally, a flickermeter model has been developed according to IEC 61000-4-15 [6].

5.2 Wind to grid model

5.2.1 Model overview

The wind to grid model covers the system from wind to grid, including wind model, aerodynamical model, drive train elasticity, generator dynamics, compensation unit and a grid model.

The wind to grid model has been developed in a reduced version using a base compensation unit, which is constantly connected and a dynamic step, which is switched in and out to control reactive power consumption from the grid. The main reason to keep the model reduced is that it already in the reduced version simulates quite slowly (approximately 10 × real time), which seems to be an inevitable consequence of using Matlab/Simulink with standard blocks and abc models for the electrical part.

Figure 31 shows the block diagram of the reduced wind to grid model. It is built in blocks, each block representing a part of the system. The blue blocks (wind model, aerodynamic model, drive train model and induction generator model) have been taken directly from the simulation platform, and are documented in [4]. The yellow blocks (grid, base compensation, compensation step, controller and Qmeas) have been developed in the present project, and are documented in the following sections. The white blocks simply copies the simulated values from Simulink to files, from which they are loaded back to Matlab for further analyses.

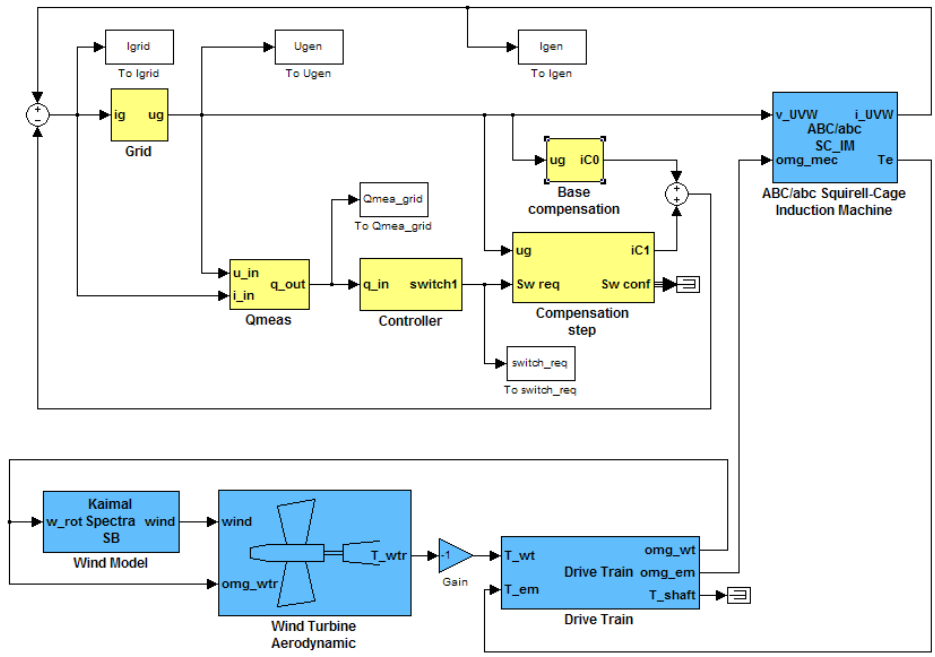

Figure 31: Overall wind to grid model

The electrical part of the system is implemented as an abc model. Thus, all voltages and currents shown in Figure 31 represent 3 phase instantaneous values.

From Figure 31 it is seen that the grid model takes the grid currents *ig* as input and provides grid voltages *ug* as output. *ug* and *ig* refer to the wind turbine 690 V terminal. The grid terminal voltages *ug* are used as input to generator and capacitor models, which then gives the currents to feed back to the grid model. The current, witch is fed back, is calculated as generator currents *i_UVW* (generation sign) minus compensation currents *iC0+iC1* (consumption sign).

The controller block sends a logical signal (switch1) to the compensation step to request switch in or out the step. Like the actual Mita-Teknik compensation step, the step confirms (Sw conf) when all three phases have been switched on, which can be used by an advanced control. However, the simulated reduced controller does not use the confirmation.

The control is based on a measured reactive power on the grid connection point. The reactive power is calculated and filtered in the *Qmeas* block.

The mechanical drive train model uses aerodynamical and electrical torque as inputs, and outputs the speeds of shaft and generator. Finally, the wind model takes the rotor speed as input, which is because it includes rotational sampling of wind speeds by 3 blades.

5.2.2 Algebraic loops

This structure of the block diagram has caused some problems with algebraic loops in the simulations, which cause the simulation to slow down and sometime even halts simulations. Particularly, the problem occurs when linear dynamic component models are simulated together with discrete components, typically for control as applied here. The problems had to be solved applying more or less physically motivated modifications of the model as discussed in the individual subsections below.

The algebraic loops basically occur when the transfer through a block is not limited at infinite frequency by the block model. An illustrative example is the capacitor and grid models applied in Figure 31. An ideal capacitor with input voltage step would result in infinite output current. Likewise, a typical inductive grid, excited by a current step, would respond with infinite voltages. Thus both these blocks have a differential behavior, which causes infinite amplification from input to output.

Generally the algebraic loops can be removed applying additional low pass filtering in the blocks. All physical systems have a low pass filter at some cut-off frequency, which limits the amplification for infinite frequencies. However, the physical cut-off frequency can be quite high, resulting in low simulation time steps and consequently very slow simulations. In that case, a lower cut-off frequency can be selected to speed up simulation, but then there is a risk to remove actual transients.

In the example with the capacitor and the inductive grid, the algebraic could be removed by integrating the ideal capacitor in the inductive grid model block, which would result in a new block with a transfer function from currents to voltages, which limits amplification of high frequencies. Thus, the algebraic loops are a consequence of the selected block structure rather than the physics, which the models describe.

However, to keep the block structure with one block representing each physical component (generator, capacitor, grid etc.), it is necessary to ensure that each block limits transfer at high frequencies. This problem becomes even stronger for an abc model trying to model the transients. The ideal model would only use small time steps when transients occur, but because of the selected high cut-off frequencies, the simulations will generally be slowed down.

5.2.3 Grid model

The Aalborg University simulation platform models in Matlab/Simulink provide separate models of transformers and of grid. The grid model applied in this project has been comprised to include a reduced model for the two transformers in addition to the 10 kV grid (see connection diagram in Figure 1). The winding resistances and the leakage reactance's of the two transformers are included in the *Rg* and *Lg* values together with the resistance and reactance representing the 10 kV grid. *u0* is an ideal voltage with constant amplitude and 50 Hz sinus.

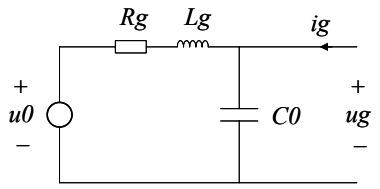

Figure 32: Single line equivalent of grid model

It is seen that the main reactance's of the transformers are omitted as they are expected to have very little influence on the reactive power control performed on the 690 V terminals.

On the other hand, a capacitance *C0* is included. This is to avoid algebraic loops. *C0=C* in (1) has been selected to provide a cut-off frequency *f*=1000 Hz, inserting *L=Lg*. The capacitance can somehow be justified by cables and busbars. However, the value of the capacitance is selected to obtain an operational cut-off frequency, which is obviously a more practical than physical motivated approach.

Figure 33 shows the Matlab/Simulink implementation of the grid model. It is seen that the number of poles (2) exceeds the number of zeroes (0 for voltage influence ua, ub and uc, and 1 for current input i_RST) in the transfer functions. Since the number of zeroes is less than the number of poles in both transfers, the algebraic loop is avoided. If *C0* was not included, the number of poles would have been 0, and the number of zeroes would be unchanged, which would cause an algebraic loop.

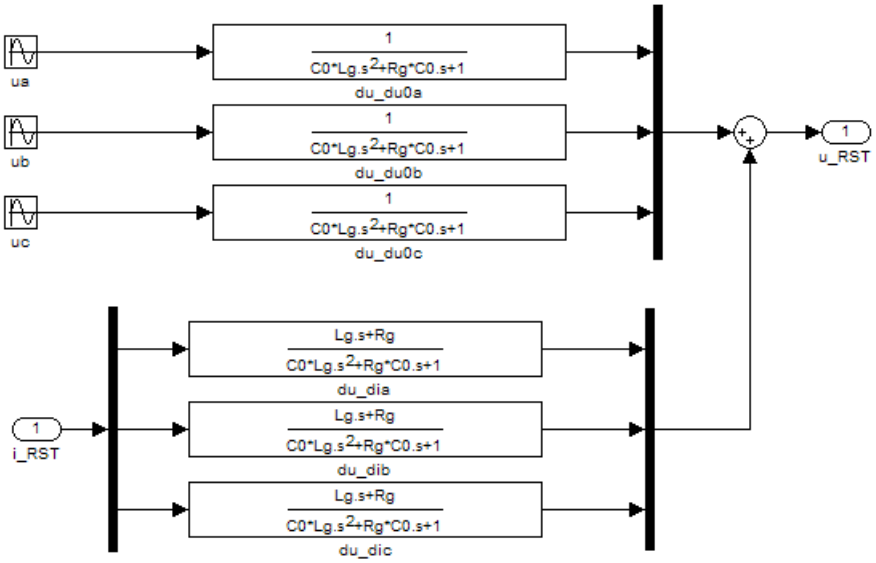

Figure 33: Grid model in Matlab/Simulink

5.2.4 Base compensation model

The base compensation is connected through the whole simulation. It represents a number of capacitor modules, typically 2 or 3, depending on the mean wind speed.

Figure 34 shows the single line equivalent for the model. *C* is the capacitance of the base compensation and *Rp* is a parallel resistance mounted to discharge the capacitor when it is not connected.

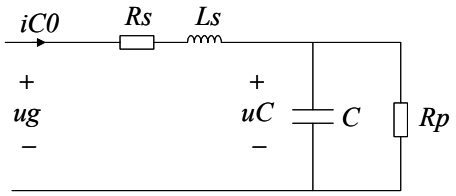

Figure 34: Single line equivalent of base compensation unit model

The thyristor voltage drop is neglected in the model. Instead, a serial inductance and a resistance are included in order to avoid algebraic loops. From the Matlab/Simulink model in Figure 35 it is seen that the number of zeroes is 1, and the number of poles is 2. If neither *Ls* nor *Rs* were included, the number of poles would be zero.

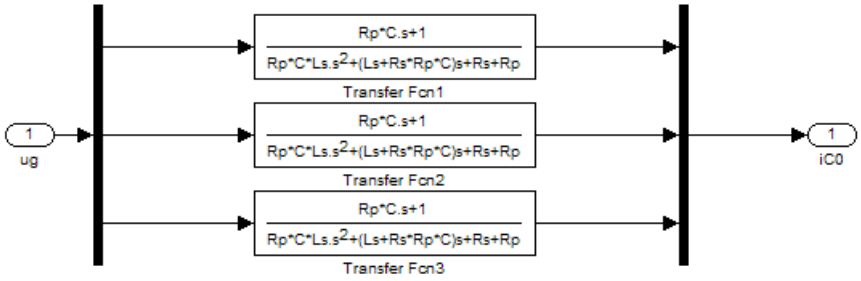

Figure 35: Base compensation model in Matlab/Simulink

5.2.5 Compensation step model

The compensation step is switched in and out during the simulation depending on the switch request from the main controller and the synchronisation control performed by the step controller. It represents a single capacitor module.

Figure 36 shows the single line equivalent for the compensation step model. It is seen to be quite similar to the base compensation model in Figure 34. Only the thyristors are included as an ideal switch *TS*, which is controlled by the module controller.

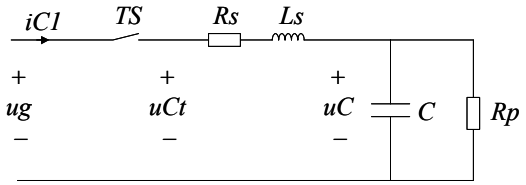

Figure 36: Single line equivalent of compensation step model

The Matlab/Simulink model first separates the voltages and currents into the individual phases as shown in Figure 37. Each phase gets the same request for switch (Swich_req), which is zero when the switch is requested open and one when the switch is requested closed. The phases return individual confirmations because the switching is done at different times for different phases, depending on the synchronisation.

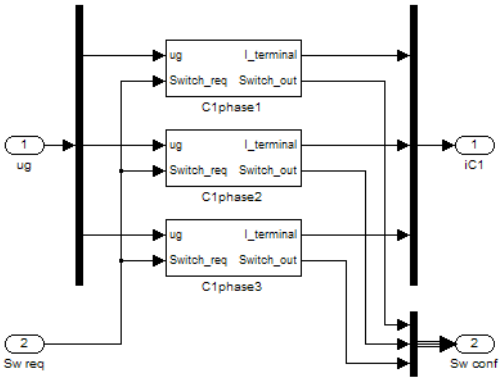

Figure 37: Phase separation in Matlab/Simulink compensation step model

Eash phase block in Figure 37 is then separated into a logical "Switch control" block and a dynamical "C-phase" block as illustrated in Figure 38. The switch control delays the switch request to the Switch_phase signal, depending on the synchronisation. The synchronisation is based on zero crossings. For switching in (close switch) the synchronisation is done when grid voltage *ug* minus capacitor voltage *uC1* is zero. For switching out (open switch) the synchronisation is done when the current *iC1* is zero.

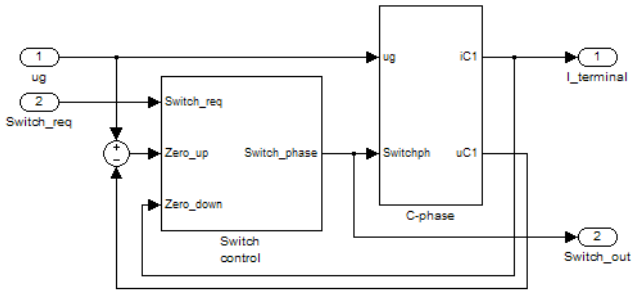

Figure 38: Single phase Matlab/Simulink blocks for module

The switch control block from Figure 38 is shown in Figure 39. The sign of the synchronisation signal (voltage difference or current) is used as trigger, i.e. the switch request is sampled and held when the sign changes. It is seen that the synchronising signals are delayed. This is necessary to avoid Matlab/Simulink solver errors. The physical delay is expected to be very small for the actual hardware, especially for opening the switch, which is done by the thyristor current zero crossing. However, a small value, larger than the smallest simulation step is needed. Consequently, the smaller delay time, the slower simulation.

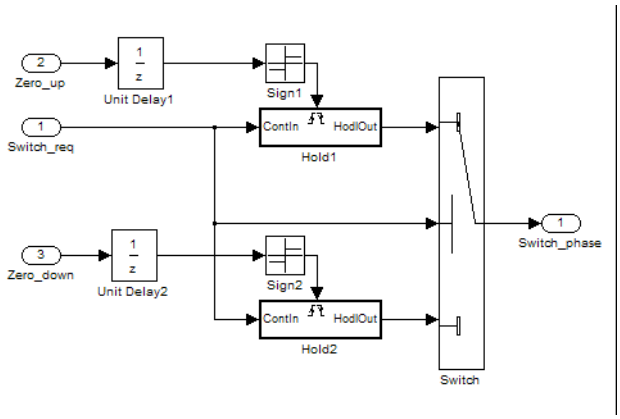

Figure 39: Single phase Matlab/Simulink blocks for module switch control)

The dynamic C-phase block from Figure 38 is shown in Figure 40. It first calculates the module phase voltage (*uCt* Figure 36) as either the grid voltage (when the switch is closed) or the discharge voltage by means of the "Integrator" (when the switch is open). The calculated module voltage is then used to calculate the module phase current *iC1* with the same dynamic equation as was used for the base compensation. Only, if the switch is open, the current is forced to zero. This forcing is necessary for numerical reasons.

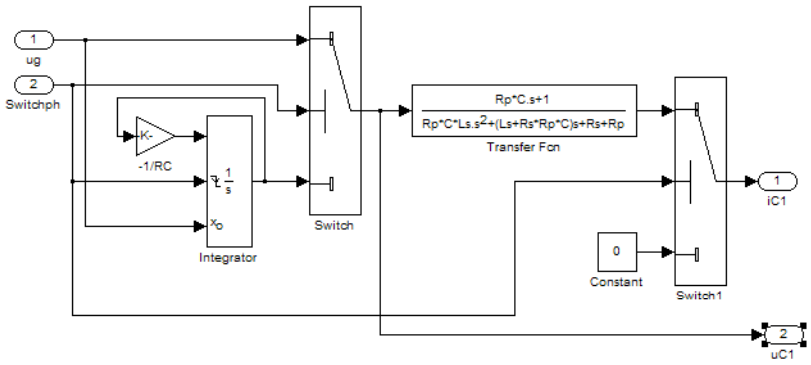

Figure 40: Single phase Matlab/Simulink blocks for module dynamics

5.3 Reduced main control

The main controller is strongly reduced in the present model, as it only controls a single module. According to Figure 31, the reduced main controller uses the reactive power measured on the grid terminals to control switching of the module. The reactive power is controlled to zero mean value, i.e. $\cos\varphi=1$.

The block diagram of the main controller is shown in Figure 41. The measured (filtered) reactive power is first sampled and held. Next, it is normalised by the gain $K=1/Q1n$, where $Q1n$ is the rated reactive power of step 1, before it is put through a relay function.

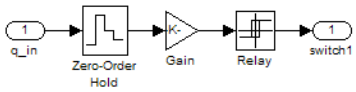

Figure 41: Main controller model

The main control model defines hysteresis as input. If the hysteresis is set to 0%, the relay will shift up when the measured reactive power exceeds $0.5\times Q1n$ and down when it exceeds $0.5\times Q1n$. If the hysteresis are set to 10%, the relay will shift up when the measured reactive power exceeds $0.6\times Q1n$ and down when it exceeds $-0.6\times Q1n$. The intension is to define the hysteresis 0% as the limit where the switch is stable (open or closed) for constant reactive power from the generator.

5.4 Reactive power measurement

The reactive power measurement in the Mita-Teknik controller is an instantaneous measurement. This ensures the fastest possible response, but it can also cause instabilities. The correct way would be to apply a filter on the instantaneous reactive power, before it is sampled and held in the main controller. This is done in the model.

Figure 42 shows the model. The instantaneous reactive power is first calculated with the standard method, where first the voltages are rotated 90 degrees using the line voltages divided by square root 3 (the gain), and then the rotated voltages are multiplied in a dot product with the currents. Then the instantaneous reactive power is filtered

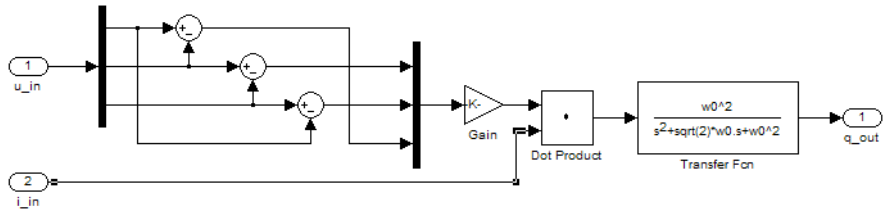

Figure 42: Reactive power measurement model

The selected method for instantaneous reactive power calculation is formally only valid for symmetrical, fundamental components of voltages and currents. However, because of the filter, possible harmonic distortion is avoided. Also the symmetry assumption is valid except for very short periods (less than one line period) where the capacitor switchings of individual phases are synchronised. Consequently, the method is acceptable for filter frequencies less than the fundamental frequency.

5.5 Flickermeter model

The flickermeter model is shown in Figure 43. It is implemented according to IEC 61000-4-15, including the 5 instantaneous outputs specified in the standard. These outputs are saved in a file during the simulation. Output 5 is the instantaneous flicker, which is used to generate short–term flicker emission (denoted

Pst), based on 10 minutes simulation. The Pst calculation is statistical, and therefore most conveniently determined after the simulation is finished.

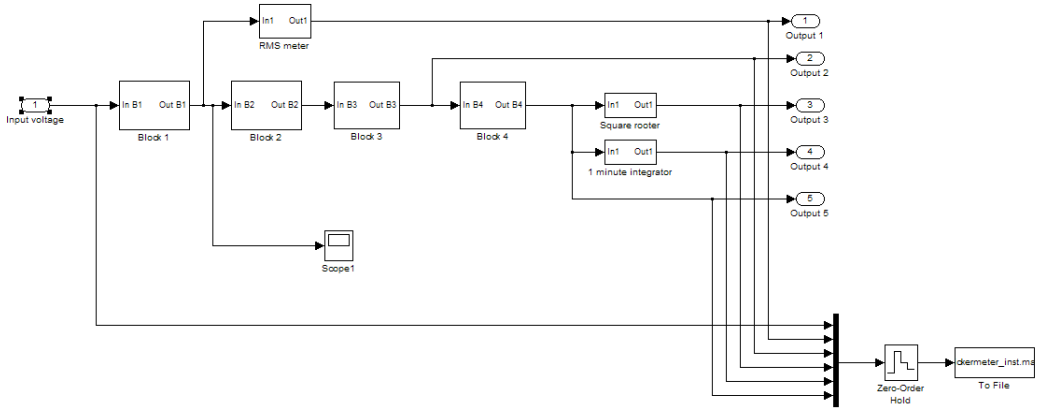

Figure 43: Flickermeter model

6 Simulation results

6.1 General

The reduction of the wind-to-grid model to a base compensation and a single controllable module has not made an ultimate verification possible. Thus, the model has not been developed to a degree, which makes it possible to compare flicker emission with different control strategies. However, the model has been tested, and some validation and verification have been done.

The compensation step model has been tested and verified against measurements in stand-alone operation of the compensation unit, and possible ways to further reduce the switching transients are analysed with the model. This is described in section 6.2.

The wind-to-grid model has also been tested. First, the operation with respect to power fluctuations is verified in section 6.3. After that, the performance of the wind-to-grid model is tested and validated in section 6.4.

6.2 Single step transients

In this section, it is described how the compensation step model has been tested and verified against the measurements presented in section 4.1, i.e. for stand-alone operation of the compensation unit. Moreover, possible ways to further reduce the switching transients are analysed with the model.

The test of the model is performed as illustrated in Figure 44. It is seen that the wind turbine including generator and the base compensation has been removed from the model compared to the complete wind-to-grid model in Figure 31. Data for the 80 kvar step has been used in the “Compenstaion step” block.

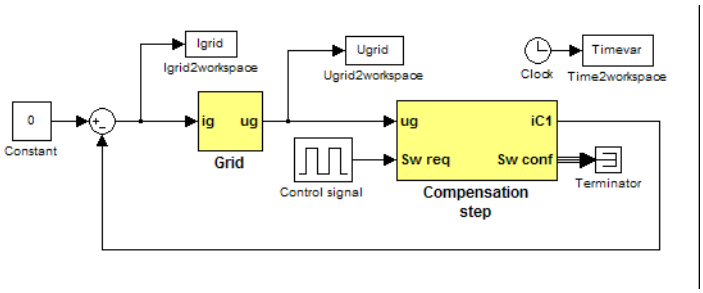

Figure 44: Capacitor step model - stand alone test

Three of the white blocks in this test simulation copies the results directly from Matlab/Simulink to the Matlab workspace for further analyses. The three selected variables are grid voltage and grid currents (which were measured in section 4.1) and the time stamp for these simulated time series. The control signal is a simple step function, where the period time, delay time and pulse width can be varied to test the capacitor switching transients.

Figure 45 shows the simulated 3 phase currents for connection of discharged 80 kvar step, and Figure 46 shows the corresponding voltages. Comparing to the measurements in Figure 5 and Figure 6, there is a quite good agreement.

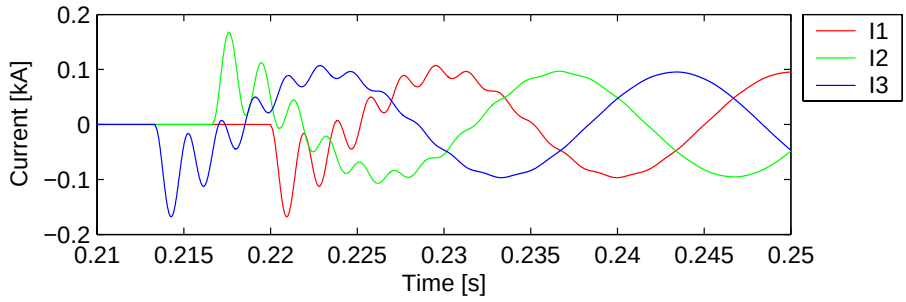

Figure 45: Simulated currents for connection of discharged 80 kvar step.

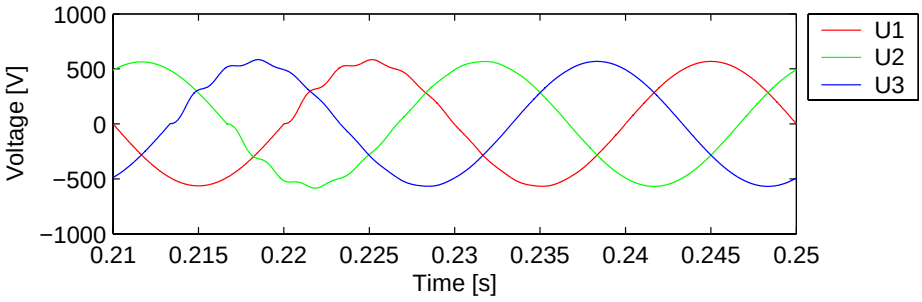

Figure 46: Simulated voltages for connection of discharged 80 kvar step.

Similar comparison has been done with an earlier version of the "Compensation step" and "Grid" models, and presented in paper [7]. The present simulations are closer to the measurements than the early version, which included neither grid capacity nor serial resistance / serial inductance in the model.

The transients are very sensitive to the serial resistance, which has been manually fitted to 0.05 ohm in Figure 45 and Figure 46. This is a relatively high contact resistance, which would cause totally 670 W heat from the 3 phases in an 80 kvar module. Thus, there is some uncertainty if this is realistic.

Another parameter which influences the transient is the serial inductance. In Figure 45 and Figure 46, the serial inductance has been chosen small to 10 μH. There is always a small inductance in a cable, and if the inductance is set to 0, a quite large, single simulation time step spike will appear on the simulated currents when the switch is closed. This can be explained by the forced delays in the simulation, and it is removed with a very small serial inductance.

It has been suggested to use a serial inductance to remove the transients in Figure 45 and Figure 46. However, simulations have shown that the transients are not removed by increasing the inductance. Only the oscillation frequency is changed. This is because the reason for the transient oscillations is actually the inductance in the grid (transformers and 10 kV grid). When the thyristor switch closes, the capacitor current tries to step up, but this is not possible if the current comes from the grid through the large reactance. Even the small simulated grid capacitance on the wind turbine side of the transformers cannot change this very much.

The only way to remove the transients seems to be to damp the oscillations with an increased serial resistance. This is illustrated in Figure 47 and Figure 48, where the serial resistance has been selected to 0.5 ohm. The transients are almost removed, and they can be completely removed by a little larger resistance. However, 0.5 ohm would cause 6.7 kW losses in a 80 kvar module, which is of course not acceptable.

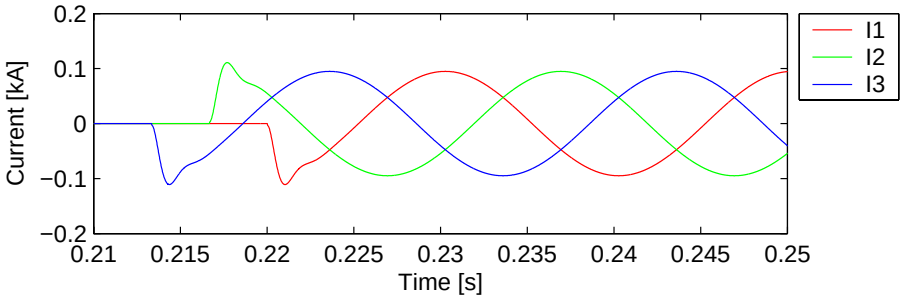

Figure 47: Simulated currents for connection of discharged 80 kvar step with high serial resistance.

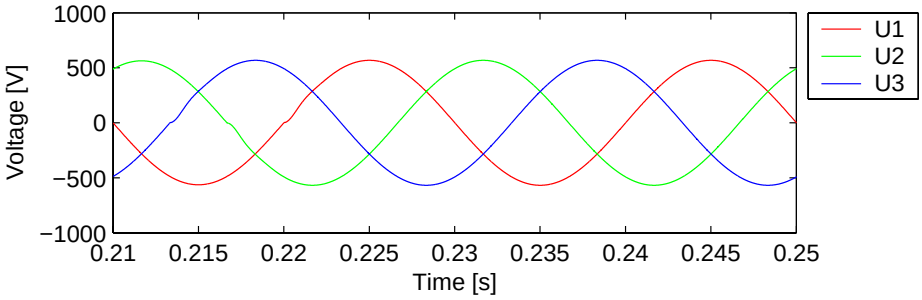

Figure 48: Simulated voltages for connection of discharged 80 kvar step with high serial resistance.

The simulation model has also been used to check the discharging. It has been shown that with the original discharge resistances Rp combined with grid data for the Risø grid connection, the 80 kvar modules need approximately 300 ms before it can reconnect. Although the time constants are smaller for the smaller capacitor steps (2 – 4 times), this may well explain why the unit is not effectively controlling every 100 ms although the controller operates with 100 ms sampling time. This simulation result lead to the installation of smaller and consequently faster discharge resistances *Rp* for the later part of the unit test.

6.3 Simulation with fixed capacitors

To validate the wind-to-grid model, test runs have been performed including only base compensation.

An example is shown in Figure 49, where 600 seconds with 10 m/s mean wind speed is simulated, and reactive power is plotted against active power. There is a good agreement compared to Figure 15. This result is a good validation of the electrical parameters for the generator model.

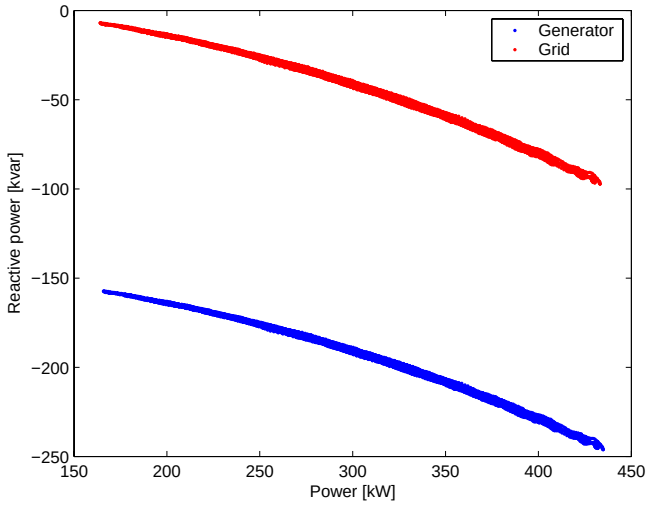

Figure 49: Reactive power of no-load compensated wind turbine, simulated with the overall wind to grid model

The PSD of the simulated power is shown in Figure 50. The shape of the PSD compares reasonably well with the measured PSD in Figure 22 up to 2 Hz. Above that, the generator frequency at 7-8 Hz is not visible in the simulation, which is similar to results with DIgSILENT simulations of continuous operation [8].

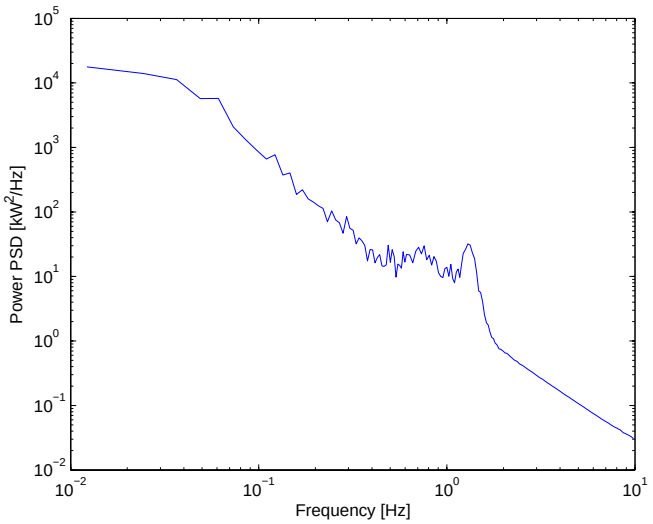

Figure 50: PSD of power simulated with the overall wind to grid model

6.4 Dynamic compensation

The wind-to-grid model has also been run in the full version shown in Figure 31, i.e. with full wind turbine model, a base compensation and a step compensa-

tion. The selected mean wind speed is 13 m/s, and the turbulence intensity is 18%. These selections provide maximum reactive power variations. The base compensation is selected to 240 kvar, representing the 3 80 kvar modules, while the step compensation is selected as the 40 kvar module.

630 seconds have been simulated totally. The maximum reactive power consumption of the generator is around 280 kvar, while minimum is below 200 kvar. A window of actual and ideal reactive power compensation is shown in Figure 51.

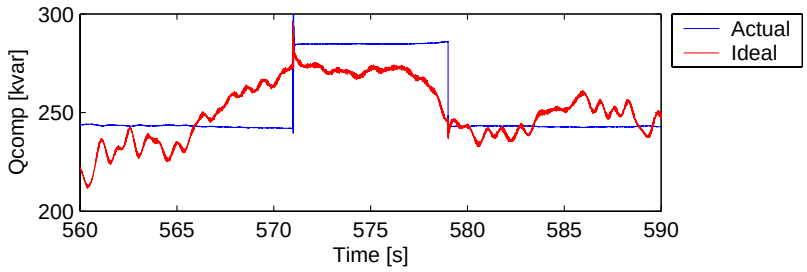

Figure 51: Window of simulated "actual" and "ideal" reactive power production from compensation unit. The "ideal" is equal to the reactive power consumed by the generator. This simulation is done with 1 s sample hold time.

It is seen that the compensation is a little behind the ideal. This is because of a combination of filter phase delay, hysteresis and control sample-hold time. The selections in Figure 51 were reactive power filter cutoff frequency 0.4 Hz, hysteresis 10 % and sample hold time 1s (i.e. 1/1s=1Hz sample frequency). Notice that the sample frequency is more than 2 times the cutoff frequency, which is the absolute minimum.

Figure 52 shows the same window with a faster controller (filter cutoff frequency 4 Hz, hysteresis 2 % and sample hold time 100ms (i.e. 10Hz sample frequency). Now it is seen that the controller shifts much faster. Another observation is that the shifts themselves cause changes in the ideal reactive power. This is because the shifts in reactive power to the grid cause voltage changes, which again cause change in the reactive power consumption of the generator.

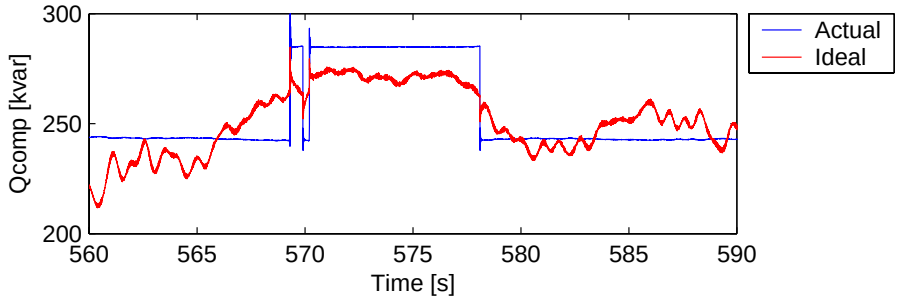

Figure 52: Window of simulated "actual" and "ideal" reactive power production from compensation unit. The "ideal" is equal to the reactive power consumed by the generator. This simulation is done with 100 ms sample hold time.

Actually, comparing Figure 52 to Figure 51 it is indicated that with the present large step, it is not optimal to run the controller so fast. At least the hysteresis should be more than 2 %.

7 Conclusions

A prototype of a dynamic phase compensation unit has been tested on the 500 kW Nordtank wind turbine in Risø, and a dynamic model has been developed, validated and partly verified. The dynamic model has also been used to support analyses, especially on the transients. The main test results are that the following:

The reactive power compensation works fine from a steady state point of view. The $\cos\varphi$ can be selected via the local display or by remote control, and the operation has been tested with power factors 0.99 and 1.00.

From a dynamic point of view, the reactive power control is capable of reducing reactive power fluctuations down to 2 Hz if the controller samples with minimum sample time (40 ms).

From a flicker point of view, the transients caused by the many capacitor switchings appear to cause more flicker than can be removed by removing reactive power fluctuations below 2 Hz. The conclusion is that with the applied control strategy, the flicker emission from the wind turbine is not reduced.

Another possible aim with the fast capacitor switchings could be to support reactive power control during grid faults. This has not been tested, and it would require a voltage dependent reactive power control. The unit could well work as standard, relatively slow compensation when the voltage is within normal range, and then switch to fast voltage support when the instantaneous voltage drops below a certain value.

From transient point of view, the switchings with thyristors have proven to strongly reduce the voltage and current transients, which occur when capacitors are switched with mechanical contactors. This is expected to ensure a much longer lifetime of switches (thyristors vs. contactors) and of capacitors.

However, measurements of the capacitance before and after the 4 months test with fast shifting frequencies have indicated that capacity has been lost, which is a sign of lifetime reduction. If the aim is to extend the lifetime of the capacitors to the full lifetime of the wind turbine, and that way to increase the reliability of the compensation, then a much slower switching frequency in normal operation is recommended. This way, the increase in flicker emission from the wind turbine, caused by capacitor switchings, could also be reduced.

Finally, the simulation models have been applied to study possible further transient reduction. Especially when a completely discharge capacitor is switched on at zero grid voltage, the capacitor current attempts to step up as it is proportional to the derived voltage. However a current step is not possible through the grid reactance, and the consequence is an oscillation with a frequency, which depends on grid inductance. Simulations have confirmed that these transient oscillations cannot be removed by a serial inductance, as this would only change the oscillation frequency.

References

[1] IEC 61400-21. Ed.1: Wind turbine generator systems – Part 21: Measurement and assessment of power quality characteristics of grid connected wind turbines. Final Draft International Standard 88/144/FDIS International Electrotechnical Commission, IEC 2001-07-01.

[2] P.Sørensen. Methods for calculation of the flicker contribution from wind turbines Risø-I-939, 1995. Risø National Laboratory, Roskilde, Denmark.

[3] P. Sørensen, A.D. Hansen, L. Janosi, B. Bak-Jensen, F. Blaabjerg, J. Bech. Simulation of wind farm interaction with grid. 2001 European wind energy conference and exhibition, Copenhagen (DK), 2-6 Jul 2001.

[4] F. Iov, F. Blaabjerg, A.D. Hansen, P. Sørensen. The Matlab/Simulink's Wind turbine blockset. General overview and Description of Models. Aalborg University, December 2003.

[5] W.Langreder. Models for Variable Speed Wind Turbines. M.Sc. Thesis, CREST Loughborough University and Risø National Laboratory, 1996.

[6] IEC 61000-4-15. Electromagnetic compatibility – Part 4: Testing and measurement techniques. Section 15: Flickermeter – Functional and design specifications.

[7] P. Sørensen, J. Skaarup, F. Iov. Dynamic phase compensation of wind turbines. Nordic Wind Power Conference, Gothenburg (SE), 1-2 Mar 2004.

[8] P. Sørensen, A.D. Hansen, L. Janosi, J. Bech, B. Bak-Jensen. Simulation of interaction between wind farm and power system. Risø-R-1281(EN) (2001)

Bibliographic Data Sheet **Risø-R-1438(EN)**

Title and authors

Test and simulation of dynamic phase compensation from Mita-Teknik A/S

Poul Sørensen, Florin Iov, Frede Blaabjerg and Jan Skaarup

ISBN	ISSN
87-550-3282-6; 87-550-3283-4 (Internet)	0106-2840

Department or group	Date
Wind Energy Department	March 2004

Groups own reg. number(s)	Project/contract No(s)
1115031-1	ENS 51171/01-0009

Pages	Tables	Illustrations	References
44	2	52	8

Abstract (max. 2000 characters)

This report describes the test of a dynamic phase compensation unit for a wind turbine with directly connected induction generators. The compensation unit is based on thyristor switched capacitors, where conventional wind turbine compensations use mechanical contactors to switch the capacitors. The influence on power quality analysed, and influence on component lifetime is discussed. Besides, simulation models in Matlab/Simulink are presented, including a flicker-meter model.

Descriptors INIS/EDB

CAPACITORS; COMPUTERIZED SIMULATION; ELECTRICAL TRANSIENTS; INDUCTION GENERATORS; POWER FACTOR; TESTING; THYRISTORS; WIND POWER PLANTS